RSC Advances

PAPER

Cite this: *RSC Adv.*, 2015, **5**, 103131

Novel metal chelators thiosemicarbazones with activity at the σ_2 receptors and P-glycoprotein: an innovative strategy for resistant tumor treatment†

Maria Laura Pati,‡[ab] Mauro Niso,‡[a] Savina Ferorelli,[a] Carmen Abate*[a] and Francesco Berardi[a]

Received 25th September 2015
Accepted 25th November 2015

DOI: 10.1039/c5ra19857g

www.rsc.org/advances

To combat the emergence of drug-resistance in tumors novel strategies are urgently needed. With this in mind we designed a novel class of thiosemicarbazones able to target simultaneously σ_2 receptors and P-glycoprotein efflux pump while chelating metals such as iron. The combined effect of these targets would lead to the activation of multiple pathways to which resistant tumors are sensitive. Indeed, most of the novel thiosemicarbazones displayed antiproliferative activity in both parent (MCF7 breast adenocarcinoma and A549 lung carcinoma) and corresponding doxorubicin-resistant cells (MCF7dx and A549dx). A few compounds emerged for their potent antiproliferative activity or for their more potent effect in doxorubicin-resistant cells than in the parent ones, while other compounds emerged for their remarkable P-gp modulatory activity. These results pave the way for further studies on these targets in the oncology field, while the availability of promising molecules for resistant tumors treatment that warrant deeper investigations was increased.

1. Introduction

After a first characterization as subtype of opiate receptors, sigma (σ) proteins were identified as a distinct class of opiate receptors divided in two subtypes, namely σ_1 and σ_2.[1] Soon thereafter σ_1 subtype was cloned from a number of species.[2] The intense research that followed has identified the σ_1 receptor as an endoplasmic reticulum chaperone involved in important brain functions. Besides implications in schizophrenia, anxiety, depression, and drug addiction, increasing evidence is correlating this subtype with neurodegenerative disorders such as Alzheimer's disease[3–5] and amyotrophic lateral sclerosis.[6,7] Moreover, important roles in modulating microglia response to brain injuries were recently shown.[8,9] All of these pieces of evidence together make σ_1 receptor a promising target for therapeutic approaches to brain diseases. Knowledge about the σ_2 receptor subtype is more incomplete. The molecular identity of the protein is still unclear, despite a number of attempts was carried out for its identification. A decade ago, σ_2 receptor was proposed as a histone-related protein,[10,11] and few years later it was identified as the progesterone receptor component 1 (PGRMC1) protein.[12] Although this latter hypothesis was generally accepted, a few controversies are emerging so that σ_2 subtype is still an 'enigma'.[13] Nevertheless, interest in σ_2 receptors is on the increase because of the involvement of these proteins in cell proliferation. Overexpression of σ_2 receptor has been found in a number of human peripheral and brain cancers, and σ_2 receptor density is higher in proliferating than in quiescent tumor cells. Therefore, this subtype has been proposed as biomarker for the proliferative status of tumors so that a number of σ_2 radioligands has been synthesized,[14,15] and a few entered clinical trials for the detection of human tumors.[16,17] Besides the diagnostic perspective, σ_2 receptors are endowed with therapeutic potentials since they show antitumor properties. σ_2 agonists exert antiproliferative action in tumor cells *in vitro*[18] as well as in preclinical tumor xenografts *in vivo*.[19,20] Several σ_2 receptor ligands with diverse structures have been developed during the years,[21] pharmacophoric models have been generated[22,23] and tools to study σ_2 receptors at the cellular level, such as fluorescent ligands have been produced.[24–30] The mechanisms of cell death activated by σ_2 receptor agonists are still under investigation and involve caspase-dependent and -independent apoptosis, generation of reactive oxygen species (ROS), and autophagy.[31,32] Curiously, the activated pathways depend on the σ_2 ligand and on the cell type, but we are still far from a clear understanding of the σ_2-mediated mechanism of action. In our

[a]*Dipartimento di Farmacia-Scienze del Farmaco, Università degli Studi di Bari ALDO MORO, Via Orabona 4, I-70125 Bari, Italy. E-mail: carmen.abate@uniba.it; Fax: +39-080-5442231; Tel: +39-080-5442750*

[b]*Division of Hepatobiliary, Pancreatic, and Gastrointestinal Surgery, Department of Surgery, Washington University School of Medicine, St. Louis, MO, USA*

† Electronic supplementary information (ESI) available: Synthesis of intermediate compounds **3**; ferrozine assay with compound **7a** and **7b** (Fig. S1); σ_2 receptor density in tumor cell lines (Table S1); description of saturation binding assay; description of detection of ROS by DCF assay and corresponding figure (Fig. S2). See DOI: 10.1039/c5ra19857g

‡ Equally contributing authors.

continuous effort to produce σ_2 receptor agonists, we recently obtained a series of σ_2 ligands with important antiproliferative activity in human MCF7 breast adenocarcinoma cells.[33] Most of the compounds displayed similar activity in the corresponding doxorubicin-resistant cell line (MCF7dx), and some of them such as siramesine (**1**, Fig. 1) and 9-[4-(6,7-dimethoxy-1,2,3,4-tetrahydroisoquinolin-2-yl)butyl]-9*H*-carbazole (**2**, Fig. 1) were even more potent in MCFdx than in MCF7 cells showing a property known as 'collateral sensitivity' (CS).[33,34] We found out that the compounds endowed with CS were also substrates of the efflux pump P-glycoprotein (P-gp) that is the mainly responsible of the Multi Drug Resistance (MDR) phenomenon. This pump is able to efflux a variety of anticancer drug and its presence has been shown to correlate with poor tumor patient prognosis, so that its clinical relevance is big. Many efforts have been devoted to the identification of selective P-gp ligands able to block the pump and restore the chemotherapeutic activity. However, such strategy that looked promising *in vitro*, failed in the clinic and alternative approaches to overcome the emergence of MDR are urgently needed. CS is an intriguing property to be investigated as a strategy for MDR tumors treatment. Different hypotheses have been formulated to justify the CS phenomenon. In accordance with one of these hypotheses, treatment of cells with P-gp substrates that are actively effluxed, would lead to ATP depletion and subsequent increase in ROS production leading to higher sensitivity to changes in energy levels.[35,36] However, interaction with P-gp is not a requirement for the compounds to retain CS, although the activity of the known CS agents is proportional to P-gp density within the cells. Indeed, CS agents have been found among compounds that do not directly interact with P-gp. Generally, these compounds are able to alter the energy equilibrium of cells, hyper-sensitizing them to ROS. Compounds such as chelators of metals that can cycle between two red-ox states (*e.g.* iron II/III, copper I/II) are among them.[35–38] All of these pieces of evidence together, prompted us to design a novel class of possible anti-tumor agents active also in resistant tumors. With this aim, we combined in one structure the σ_2 pharmacophore and the P-gp directing portion together with a metal chelating moiety. The 6,7-dimethoxy-1,2,3,4-tetrahydroisoquinoline or 1-cyclohexylpiperazine basic moieties were linked through a butyl chain to the isatin-*N*-atom in order to build the σ_2 receptor and P-gp directing portion, while the metal chelation property was obtained by functionalizing the isatin nucleus to a thiosemicarbazone moiety. The combined results from this study suggest that the proposed multitarget strategy is promising for resistant tumors treatment. Despite the absence of potent CS agents, some of the novel thiosemicarbazones show important antiproliferative activity in both parent and doxorubicin resistant cells, and a few hold promises for resistant tumors treatment warranting further investigation.

2. Results and discussion

2.1. Chemistry

The synthetic pathway for the synthesis of final compounds is depicted in Scheme 1. Upon alkylation of isatin with 1-bromo-4-chlorobutane in the presence of K_2CO_3, intermediate chlorobutyl **3** was obtained. Compound **3** was then used to alkylate either 6,7-dimethoxy-1,2,3,4-tetrahydroisoquinoline or 1-cyclohexylpiperazine in the presence of K_2CO_3 to produce either **4a** or **4b**. These two intermediate amines were transformed into their corresponding hydrochloride salts, dissolved in hot EtOH and treated with the appropriate thiosemicarbazides to afford final thiosemicarbazones **5a**,**b**–**17a**,**b** as hydrochloride salts (Table 1).

2.2. Biology

2.2.1. σ_2 receptor binding. Results from binding assays for all the novel compounds are expressed as inhibition constants (K_i values) in Table 1. The novel thiosemicarbazones displayed nanomolar affinities comparable to those of lead compound siramesine **1** with K_i values ranging from 7.03 nM to 35.4 nM. There were no appreciable differences between the affinity values of 6,7-dimethoxytetrahydroisoquinoline and cyclohexylpiperazine derivatives, and as already demonstrated with other structures (*e.g.* tetralin, indole, carbazole, benzamide compounds), the two basic moieties were confirmed to be useful to confer high σ_2 receptor affinity also in these isatin-thiosemicarbazone-based structures.[14,33,39–41] In the 6,7-dimethoxytetrahydroisoquinoline series, the absence of a substituent (**5a**) or the presence of a small or bulkier group at the thiosemicarbazone

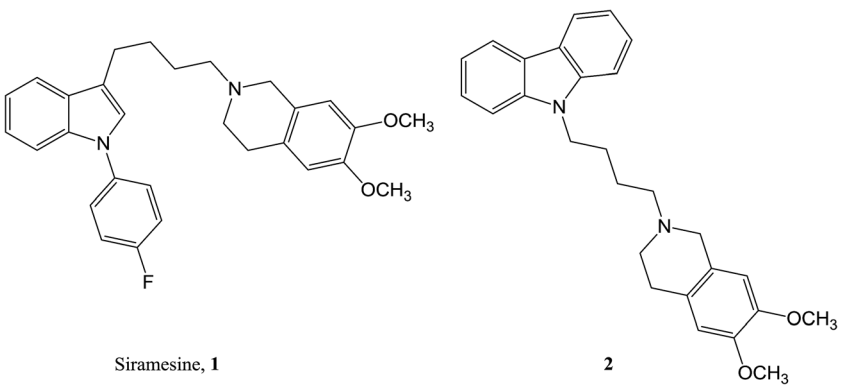

Siramesine, **1** **2**

Fig. 1 Reference σ_2 ligands.

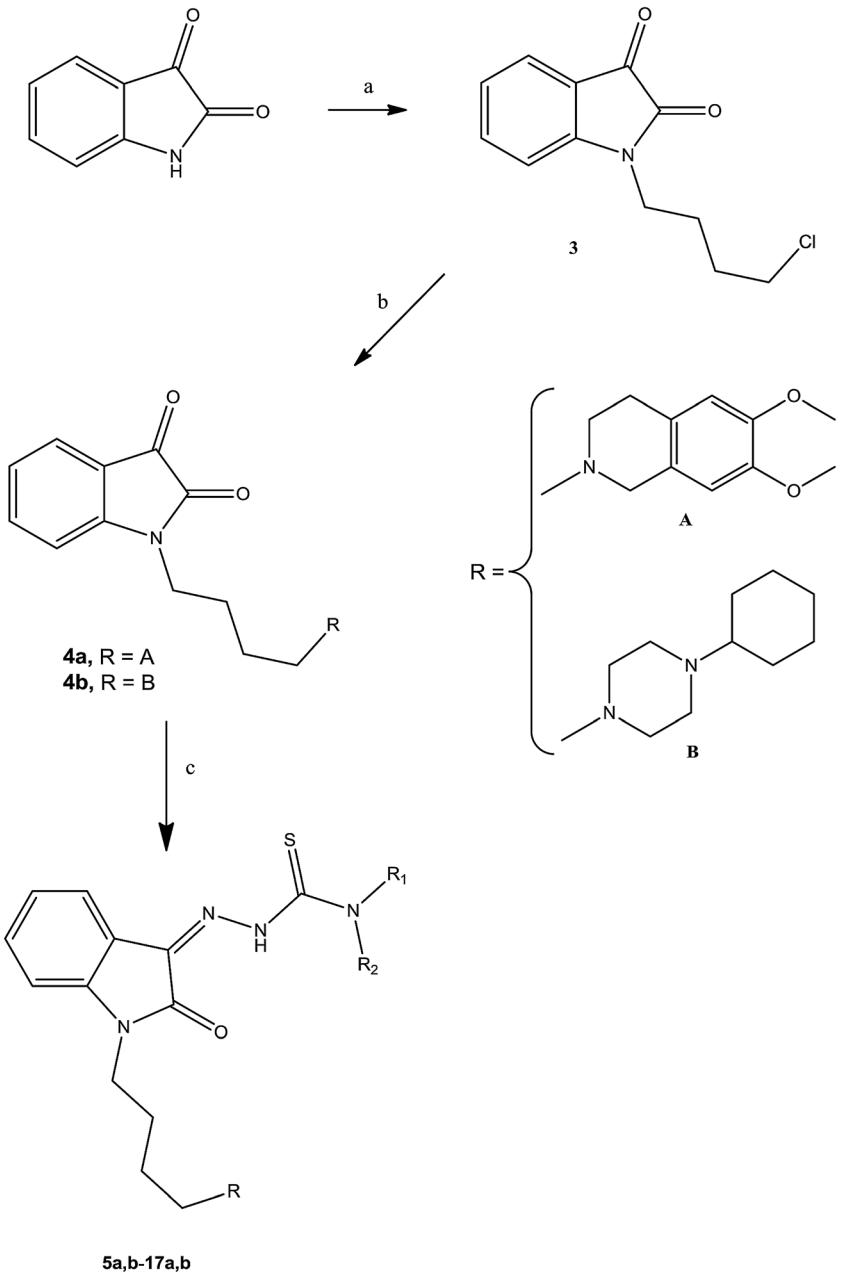

Scheme 1 Reagents: (a) $Br(CH_2)_4Cl$, K_2CO_3, CH_3CN; (b) 6,7-dimethoxy-1,2,3,4-tetrahydroisoquinoline or 1-cyclohexylpiperazine, K_2CO_3, CH_3CN; (c) appropriate thiosemicarbazide, EtOH.

moiety, such as methyl (**6a**), i-propyl (**8a**), *t*-butyl (**9a**), benzyl (**10a**) or 1-naphthyl (**17a**) determined high affinity binding at the σ_2 receptor ($K_i = 7.03$ nM, $K_i = 15.9$ nM, $K_i = 8.70$ nM, $K_i = 7.65$ nM, $K_i = 9.90$ nM and $K_i = 7.20$ nM; respectively). These data suggested the presence of a region of tolerance in the portion of the σ_2 receptor binding site that accommodates the thiosemicarbazone moieties. A further support to this 'tolerance region' was given by the phenyl substitution at the thiosemicarbazone moiety. The phenyl ring (**11a**) determined a lower but still notable interaction with the σ_2 binding site ($K_i = 19.1$ nM), and the insertion of an electron-withdrawing (F, Cl, CF_3) or -donating (CH_3, OCH_3) substituents in the *para* position of the phenyl ring did not influence the affinity at the σ_2 receptor (K_i values ranging from 14.7 nM to 20.8 nM), with no substituent effect. On the other hand, the bis-methyl substitution on the thiosemicarbazone group in the 6,7-dimethoxytetrahydroisoquinoline derivatives led to the lowest σ_2 receptor affinity of the series (**7a**; $K_i = 34.1$ nM). Results from the cyclohexylpiperazine series were in accordance with results from the 6,7-dimethoxytetrahydroisoquinoline one. The absence of a substituent (**5b**) or the presence of one methyl (**6b**), i-propyl (**8b**), *t*-butyl (**9b**) or benzyl group (**10b**) as well as a phenyl substituent (**11b**) on the thiosemicarbazone moiety determined similar σ_2 receptor binding ($K_i = 14.8$ nM, 27.1 nM, 28.0 nM, 23.2 nM, 17.2 nM, and 16.4 nM; respectively). Also in this class, the aryl

Table 1 Biological data of novel thiosemicarbazone derivatives

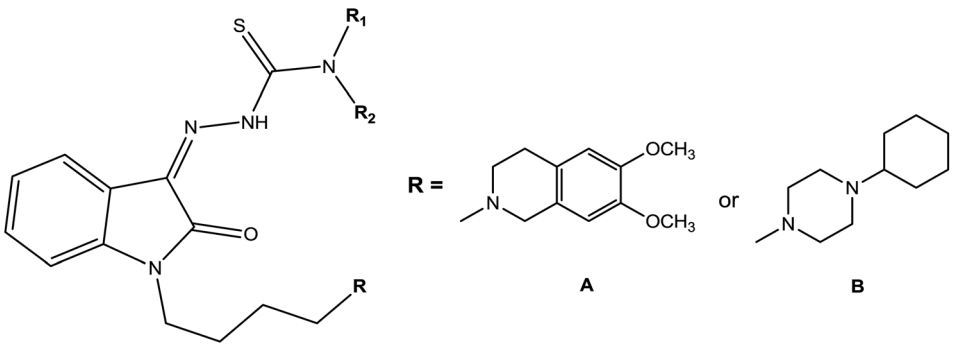

				$K_i \pm SEM^a$ (nM)	$EC_{50} \pm SEM^a$ (μM)					
Cpd	R	R_1	R_2	σ_2	MCF7	MCF7dx	A549	A549dx	Calcein-AM	ATP[b]
1, siramesine				12.6[c]	12.3[c]	5.90[c]	15.4[d]	4.63[d]	1.41[c]	Yes
2				0.04[c]	28.2[c]	17.1[c]	26.4[d]	11.7[d]	0.42[c]	Yes
5a	A	H	H	7.03 ± 1.8	>100	>100	>100	>100	0.24 ± 0.02	No
5b	B			14.8 ± 3.1	>100	>100	>100	>100	2.95 ± 0.3	No
6a	A	CH_3	H	15.9 ± 4.2	>100	78.4 ± 1.0	33.9 ± 6.1	37.2 ± 2.5	0.11 ± 0.03	No
6b	B			27.1 ± 3.8	52.6 ± 5.5	77.6 ± 1.3	>100	61.8 ± 1.7	0.65 ± 0.12	No
7a	A	CH_3	CH_3	34.1 ± 5.1	24.6 ± 3.6	15.7 ± 1.6	10.4 ± 1.6	3.89 ± 0.5	3.04 ± 0.18	No
7b	B			35.4 ± 8.8	1.81 ± 0.4	2.95 ± 0.4	2.20 ± 0.3	2.83 ± 0.4	2.83 ± 0.35	No
8a	A		H	8.70 ± 1.5	25.9 ± 0.7	22 ± 0.3	20.7 ± 1.2	19.4 ± 1.2	0.075 ± 0.01	No
8b	B			28.0 ± 4.3	17.6 ± 0.8	25.0 ± 1.6	29.0 ± 5.5	28.1 ± 3.1	0.45 ± 0.05	No
9a	A		H	7.65 ± 2.0	18.0 ± 1.4	20.3 ± 1.0	16.1 ± 0.4	16.7 ± 1.2	0.32 ± 0.03	No
9b	B			23.2 ± 2.2	7.67 ± 0.2	17.4 ± 1.3	13.0 ± 1.7	14.6 ± 1.2	0.98 ± 0.06	Yes
10a	A	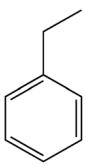	H	9.9 ± 1.0	>100	>100	20.6 ± 4.0	13.3 ± 1.9	0.065 ± 0.03	No
10b	B			17.2 ± 2.1	18.5 ± 0.1	20.2 ± 0.2	16.8 ± 0.3	14.8 ± 0.7	0.84 ± 0.1	Yes
11a	A	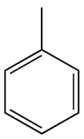	H	19.1 ± 1.4	>100	>100	>100	61.3 ± 1.6	0.35 ± 0.03	No
11b	B			16.4 ± 2.5	12.5 ± 2.6	18.6 ± 0.5	11.5 ± 1.8	10.9 ± 1.4	1.28 ± 0.2	Yes
12a	A	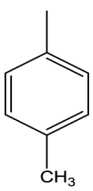	H	20.8 ± 3.3	>100	>100	>100	52.6 ± 8.7	0.38 ± 0.05	No
12b	B			14.7 ± 0.5	16.0 ± 2.3	17.2 ± 1.5	6.68 ± 1.1	6.02 ± 0.2	1.82 ± 0.15	Yes
13a	A	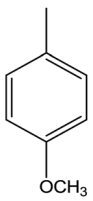	H	16.4 ± 1.2	>100	>100	>100	>100	0.22 ± 0.05	No
13b	B			16.8 ± 1.7	14.6 ± 0.5	12.4 ± 2.8	13.4 ± 2.6	14.1 ± 1.6	0.88 ± 0.1	Yes

Table 1 (*Contd.*)

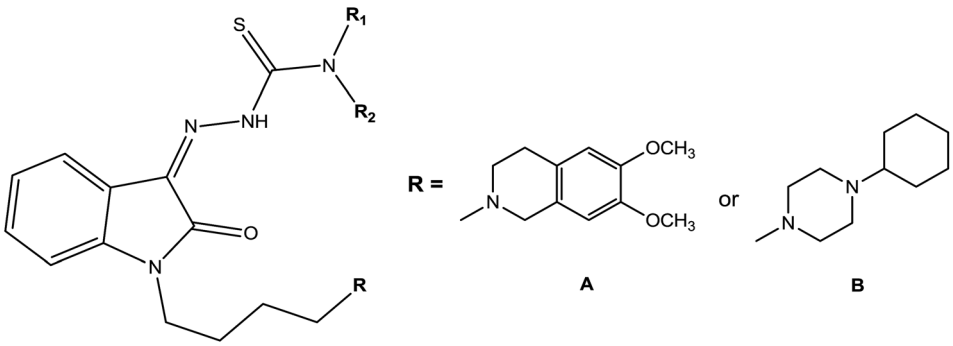

				$K_i \pm$ SEM[a] (nM)	$EC_{50} \pm$ SEM[a] (μM)					
Cpd	R	R_1	R_2	σ_2	MCF7	MCF7dx	A549	A549dx	Calcein-AM	ATP[b]
14a	A	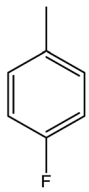	H	14.9 ± 2.0	>100	34.3 ± 0.5	16.7 ± 0.5	12.4 ± 1.0	0.28 ± 0.05	No
14b	B			28.2 ± 3.1	14.9 ± 1.4	21.3 ± 2.6	8.78 ± 1.6	10.4 ± 1.4	1.42 ± 0.3	Yes
15a	A	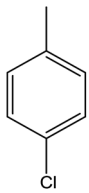	H	19.1 ± 1.9	>100	45.9 ± 0.5	19.8 ± 1.2	22.6 ± 1.7	0.80 ± 0.1	No
15b	B			22.2 ± 2.6	12.6 ± 1.1	21.5 ± 1.0	10.8 ± 2.1	6.54 ± 0.5	2.45 ± 0.60	Yes
16a	A	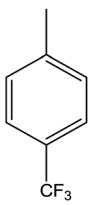	H	14.7 ± 1.3	>100	>100	>100	>100	0.47 ± 0.03	No
16b	B			14.2 ± 1.5	19.0 ± 1.2	17.9 ± 0.9	15.5 ± 0.5	15.7 ± 2.4	4.21 ± 0.8	Yes
17a	A	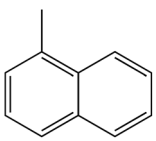	H	7.20 ± 0.16	>100	>100	>100	>100	0.04 ± 0.001	No
17b	B			15.2 ± 2.1	15.8 ± 1.5	18.8 ± 0.6	10.1 ± 0.4	12.0 ± 0.1	0.91 ± 0.07	Yes
DTG				25.7 ± 1.41						

[a] Values represent the mean of $n \geq 2$ separate experiments in duplicate ± SEM. [b] 'Yes': ATP is depleted, 'No': ATP is not depleted. [c] From ref. 33. [d] From ref. 34.

substitution on the thiosemicarbazone did not appear to suffer from steric or electronic effects. 1-Naphthyl-bearing thiosemicarbazone (**17b**) was one among the highest σ_2 affinity ligands within the cyclohexylpiperazine series (K_i = 15.2 nM), and in the *para*-substituted phenyl derivatives, the methyl (**12b**), methoxy (**13b**) trifluoromethyl (**16b**), fluoro (**14b**) or chloro (**15b**) substitution determined similar σ_2 binding affinities (K_i values = 14.7 nM, 16.8 nM, 14.2 nM, 28.2 nM, and 22.2 nM; respectively). Also in this class of compounds, the presence of the bis-methyl group on the thiosemicarbazone moiety (**7b**) led to the highest K_i value of the series (K_i = 35.4 nM), so that the bis-substitution appears to be detrimental for high-affinity interaction at σ_2 receptor in the thiosemicarbazone derivatives series.

2.2.2. Calcein-AM and ATP-depleting assays. The interaction of these compounds with P-gp was evaluated through the calcein-AM assay in combination with the ATP-depleting assay. Results are reported in Table 1 as EC_{50} for the calcein-AM assay and as 'Not' (ATP is not depleted) or 'Yes' (ATP is depleted) for the ATP-depleting assay. In contrast to other already known isatin-β-thiosemicarbazones devoid of the σ_2/P-gp targeting moieties

such as the *N*-butyl-6,7-dimethoxytetrahydroisoquinoline and *N*-butyl-1-cyclohexylpiperazine,[42] all of the novel compounds interacted with P-gp from the low micromolar to sub-micromolar range. 6,7-Dimethoxytetrahydroisoquinoline derivatives displayed a noticeable and more potent interaction with P-gp in comparison to the corresponding 1-cyclohexylpiperazine counterparts (from 3- to 20-fold more potent), all with EC_{50} values below 1 μM. The only exception was the dimethyl-substituted derivative (**7a**) which displayed the highest EC_{50} value (3.04 μM) suggesting that the double substitution at the thiosemicarbazone moiety is also detrimental for P-gp interaction in the 6,7-dimethoxytetrahydroisoquinoline derivatives. The absence of a substituent at the thiosemicarbazone moiety (**5a**) or the presence of a mono-methyl (**6a**), *t*-butyl (**9a**), and the phenyl (**11a**) (EC_{50} values = 0.24 μM, 0.11 μM, 0.32 μM, 0.35 μM; respectively) substitution determined a strong P-gp interaction. The presence of electron-withdrawing or -donating groups in the *para* position of the phenyl ring did not affect interaction with the P-gp (EC_{50} values ranging from 0.22 μM to 0.80 μM) in agreement with the interaction of these compounds with the σ_2 receptors. The P-gp activity determined by moieties such as i-propyl (**8a**; $EC_{50} = 0.075$ μM), benzyl (**10a**; $EC_{50} = 0.065$ μM) and 1-naphthyl (**17a**; $EC_{50} = 0.04$ μM) are worthy of note since they reached the submicromolar EC_{50} values of the most potent P-gp ligands known. Unexpectedly, all of the 6,7-dimethoxytetrahydroisoquinoline derivatives were not actively effluxed by P-gp as they do not increase the ATP depletion in the cells studied, in contrast to reference compounds **1** and **2**. Nevertheless, while these compounds cannot activate the futile ATP-cycle, they may block P-gp allowing their entrance into the cells where the antiproliferative activity can be exerted. As for 1-cyclohexylpiperazine derivatives, EC_{50} values ranged from 0.45 μM to 4.21 μM. In this series, the absence of a substituent at the thiosemicarbazone moiety (**5b**) or the presence of a di-methyl one (**7b**) led to the same degree of P-gp modulation (EC_{50} = 2.83 μM and 2.95 μM, respectively), whereas the mono-methyl (**6b**) and the i-propyl (**8b**) substitutions led to a more potent activity (EC_{50} = 0.65 μM and 0.45 μM, respectively). These four molecules did not increase ATP depletion, whereas all of the other 1-cyclohexylpiperazine derivatives, bearing *t*-butyl (**9b**), benzyl (**10b**) or aryl (**11b–17b**) groups, determined an increase in ATP depletion, suggesting an active efflux of the compounds out of the cells with the possible activation of the futile ATP-cycle. As already verified, small changes in the structures of P-gp modulators are able to modify the interaction mechanism at the P-gp pump,[43] with the *t*-butyl substituted derivative (**9b**) depleting ATP in contrast to the i-propyl substituted one (**8b**). Also in the cyclohexylpiperazine series, there was no electronic effect in the aryl-substituted derivatives with most of the aryl compounds presenting EC_{50} values around 1 μM. However, the fact that these aryl-substituted derivatives are ATP-depleting agents denotes a different interaction with P-gp compared to their 6,7-dimethoxytetrahydroisoquinoline counterparts.

2.2.3. Iron chelation. Isatin-β-thiosemicarbazones are known as metal chelators and they have been particularly exploited as iron chelators.[36,42] To rule out that the functionalization of the isatin-*N*-atom with the σ_2-directioning portions affects the chelation properties, the ferrozine assay was performed. In order to take into account the different structural variables, the three couples of thiosemicarbazones, **6a**/**6b**, **7a**/**7b** and **11a**/**11b**, were investigated. In this manner, the influence of the two σ_2-receptor directing moieties was coupled to the different functionalization at the thiosemicarbazone portion: mono-alkyl, di-alkyl and aryl substitution. In all of the compounds, chelation of iron II was detected to the same extent (Fig. S1, in ESI†) confirming the ability of these novel thiosemicarbazones to sequester iron species, likely altering the cell red-ox equilibrium and contributing to the antiproliferative effects of these compounds.

2.2.4. Antiproliferative activity in MCF7 and MCF7dx and in A549 and A549dx cell line pairs. The antiproliferative activities of novel and reference compounds were evaluated in two cell lines pairs: the MCF7 breast adenocarcinoma, the A549 lung carcinoma and their corresponding doxorubicin resistant MCF7dx and A549dx cell lines, where it was also verified that the overexpression of P-gp did not affect the expression of σ_2 receptors (Table S1, in ESI†). Antiproliferative activities of the compounds are expressed as EC_{50} values in Table 1. Generally, cyclohexylpiperazine derivatives were more potent than the corresponding 6,7-dimethoxytetrahydroisoquinoline ones, suggesting the importance of the basic moiety in conferring the antiproliferative action to these compounds. As for the monoalkyl substituted thiosemicarbazones, activity in both the 6,7-dimethoxytetrahydroisoquinoline (**6a**, **8a** and **9a**) and the cyclohexylpiperazine (**6b**, **8b** and **9b**) derivatives increased with the size of the alkyl group in the four cell lines, with the *t*-butyl substituent providing the lowest EC_{50} values. The absence of substituents at the thiosemicarbazone determined the lack of antiproliferative activity in all the cell lines studied, both in the 6,7-dimethoxytetrahydroisoquinoline (**5a**) and cyclohexylpiperazine (**5b**) series (EC_{50} values > 100 μM), as already verified in other cell lines for the corresponding isatin-β-thiosemicarbazone devoid of the *N*-butyl-linked basic moieties targeting σ_2 and P-gp proteins (*i.e.* 6,7-dimethoxytetrahydroisoquinoline and cyclohexylpiperazine).[36] In contrast to the σ_2 affinity and P-gp activity, the di-methyl substitution generated potent antiproliferative properties, with the 6,7-dimethoxytetrahydroisoquinoline derivative (**7a**) displaying more potent activity in the doxorubicin resistant cells (EC_{50} = 15.7 μM in MCF7dx; $EC_{50} = 3.89$ μM in A549dx), than in the parent ones ($EC_{50} = 24.6$ μM in MCF7; EC_{50} = 10.4 μM in A549), with hints of CS. The same substitution in the cyclohexylpiperazine derivatives (**7b**) determined the most potent antiproliferative activity of the whole series of thiosemicarbazones, with no differences between the parent and resistant cell lines (EC_{50} values ranging from 1.81 μM to 2.95 μM). This result is in line with already known thiosemicarbazones: despite the diverse structures of the thiosemicarbazones, the presence of the N-terminal di-methylation has often proven to enhance the antiproliferative activity.[38,44,45] A few 6,7-dimethoxytetrahydroisoquinoline derivatives were devoid of antiproliferative activity (EC_{50} values > 100 μM) in both the cell lines pairs (**5a**, **13a**, **16a**, **17a**) or in both MCF7 cell lines (**11a** and **12a**). Few other 6,7-dimethoxytetrahydroisoquinoline derivatives were devoid of activity in the parent cells, whereas they displayed a certain antiproliferative effect in the corresponding doxorubicin

resistant cells. Examples are **14a** and **15a** without effect in MCF7 cells but with antiproliferative activity in MCF7dx cells (EC_{50} = 34.3 μM and 45.9 μM, respectively), and **11a** and **12a** without activity in A549 but with a weak antiproliferative effect in A549dx (EC_{50} values of 61.3 μM and 52.6 μM, respectively). The same behavior was shown by the cyclohexylpiperazine compound **6b** that displayed weak antiproliferative activity in A549dx (EC_{50} = 61.8 μM) but not in A549 parent cells. Although clear structure activity relationships cannot be drawn for these molecules, in the cyclohexylpiperazine derivatives the substitution on the phenyl ring did not influence the antiproliferative activity. All the phenyl-bearing compounds (**11b**, **12b**, **13b**, **14b**, **15b**, and **16b**) displayed similar EC_{50} values (around 10 μM) with more potent action in A549 cells than in MCF7 cells. Also, the steric hindrance at the cyclohexylpiperazine thiosemicarbazones did not influence this trend as shown by the naphthyl (**17b**), benzyl (**10b**) and *t*-butyl (**9b**)-bearing derivatives. On the other hand, a certain dependence on the electronic effects in the aryl-substituted thiosemicarbazone derivatives was recorded in the 6,7-dimethoxytetrahydroisoquinoline compounds. A considerable improvement of the activity, particularly in the A549 cell line pairs, was recorded in the electron-withdrawing *p*-F-phenyl (**14a**) and *p*-Cl-phenyl (**15a**) thiosemicarbazone derivatives compared to the compounds bearing unsubstituted or electron rich phenyl rings (**11a**, **12a**, **13a**). Nevertheless, the more hindered electron-withdrawing *p*-CF_3-phenyl compound (**16a**) did not show any antiproliferative activity, as well as the bulky naphthyl **17a**. It must be noticed that the presence of the cyclohexylpiperazine moiety led to results in line with the antiproliferative activity exerted by the corresponding isatin-β-thiosemicarbazones devoid of the *N*-butyl-linked basic moieties which were previously produced (*i.e.* methyl, i-propyl, phenyl, benzyl and naphthyl derivatives).[36] On the other hand, the presence of the 6,7-dimethoxytetrahydroisoquinoline generally determined a reduction of the antiproliferative activity when compared to the corresponding isatin-β-thiosemicarbazone devoid of the basic moiety.[36] In particular, this was the case for the naphthyl, phenyl and benzyl derivatives. The presence of the 6,7-dimethoxytetrahydroisoquinoline completely abolished the antiproliferative activity in all the cell lines studied for the naphthyl derivative (**17a**), whereas the activity was abolished in MCF7 cell lines and partially maintained in the A549 cells pair for the benzyl (**10a**) and phenyl (**11a**) derivatives.

Curiously and in contrast to the two reference compounds **1** and **2**, none of the few compounds that depleted ATP (**9b**, **10b**, **11b**, **12b**, **13b**, **14b**, **15b**, **16b**, **17b**) exerted CS, except for **15b** that displayed a weak CS in the A549 cell line pairs. However, worthy of note is that all of the ATP-depleting agents showed important antiproliferative activity in all the four cell lines. On the other hand, the block of P-gp induced by the 'no ATP-depleting agents' may grant their entrance into the P-gp overexpressing cells allowing the activation of cell death pathways. All these results together demonstrate that the activity of these multitarget compounds is not directly related to the σ_2 receptor affinity or to the P-gp modulation activity, as it rather depends on a combination of activities at different targets, in which also off-target effects may be involved. However, combination of these activities mostly resulted in antiproliferative agents potently active in resistant tumors, in line with other thiosemicarbazones already known, with compounds **7a** and **7b** that warrant deeper investigation.

2.2.5. ROS involvement in the antiproliferative activity of 7a and 7b. The contribution of ROS generation to the antiproliferative action of the two most potent compounds, *i.e.* **7a** and **7b**, was indirectly studied by pre-administration of the lipid antioxidant α-tocopherol (100 μM) in all the four cell lines (Fig. 2). In MCF7 cells, α-tocopherol determined an important rescue of cell viability at 24 h reverting the cell death caused by **7b** administered up to 100 μM: from 75% cells surviving at **7b** administered at 10 μM, to 60% cells surviving at 30 μM **7b**, to 35% cells still surviving at 100 μM **7b**. In MCF7dx the rescue was more limited: α-tocopherol was still able to rescue cells from 10 μM **7b** (70% viability), but cell death determined by higher concentrations of **7b** was not reverted, with no differences between the α-tocopherol treated and untreated cells. The same behavior was detected with **7a**: in MCF7 cells important reversion of cell death by α-tocopherol was recorded even in the presence of 100 μM **7a** (50% viability), whereas in MCF7dx there was only a slight and not significant reversion at each concentration of **7a** used, suggesting that more α-tocopherol is needed to save MCF7dx cells from death. Very similar rescue from cell death by α-tocopherol was recorded in human A549 lung carcinoma cells and the corresponding doxorubicin-resistant A549dx. Cell death caused by **7a** and **7b** administered at 10 μM was importantly rescued by α-tocopherol in the lung cell lines, and a partial rescue from cell death was still in the two cell lines upon treatment with the compounds at 100 μM. Involvement of ROS in the antiproliferative action of these compounds was additionally confirmed by experiment with 5-(and-6)-carboxy-2′,7′-dichlorodihydro-fluorescein diacetate (carboxy-H_2DCFDA) (Fig. S2, in ESI†). These results taken together support that generation of ROS is at least partially responsible of the mechanism of action of these compounds in all the cell lines studied. However, the two cell lines pairs show different sensitivities to α-tocopherol and to these compounds, as already suggested by the results given by the thiosemicarbozones in the antiproliferative assays.

2.3. Discussion

Based on previous structural activity relationship (SAR) studies, structural features prone to target both σ_2 receptors and P-gp pump, and to chelate metals were combined in these novel thiosemicarbazones with the aim of producing potent anticancer agents also active in doxorubicin resistant cells. Most of the compounds displayed high σ_2 receptor affinity and potent P-gp modulatory activity, with the majority of them appearing as P-gp inhibitors rather than P-gp substrates as they do not increase ATP consumption, in contrast to the lead compounds **1** and **2**. Among them, there were some thiosemicarbazones devoid of antiproliferative effect, whereas all the ATP-consuming thiosemicarbazones displayed important antiproliferative action in the four cell lines studied, suggesting that ATP consumption gives a contribution to the overall effect of these multitarget

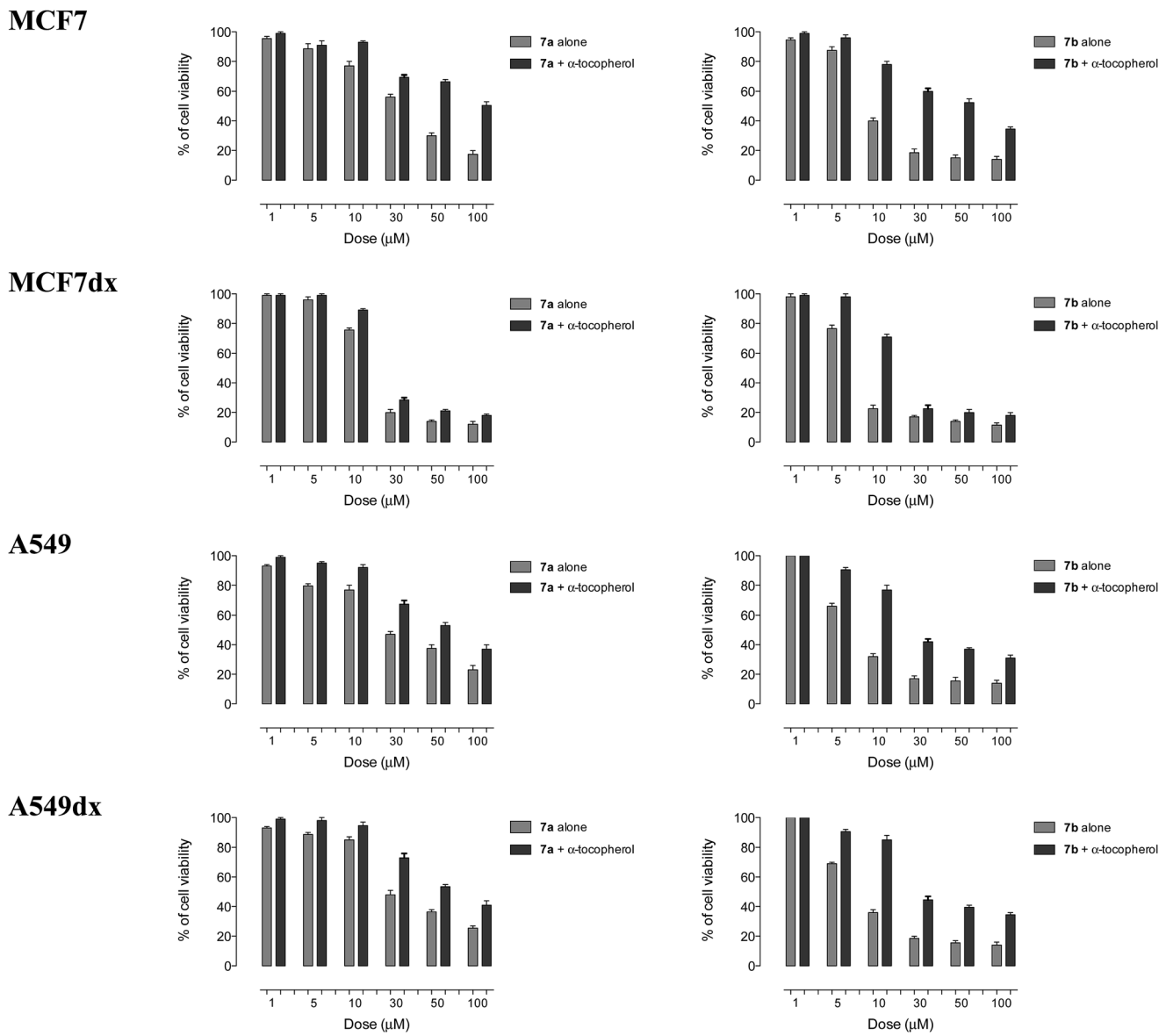

Fig. 2 Antiproliferative effect of compounds **7a** and **7b** with or without α-tocopherol (100 μM) in MCF7, MCF7dx, A549 and A549dx.

agents, although it is not determining. In fact, the cyclohexylpiperazine derivative **7b**, whose mechanism of action does not involve increase in ATP depletion, emerged as the most potent antiproliferative agent of the series, with similar and low micromolar EC_{50} values in parent and resistant cells. The corresponding 6,7-dimethoxytetrahydroisoquinoline thiosemicarbazone **7a** displayed higher activity in the resistant cells than in parent ones, particularly in the A549dx lung carcinoma cells, where a potent and 2.7-fold higher activity than in A549 cells was recorded. Curiously, these two compounds – *i.e.* **7a** and **7b** – displayed the lowest σ_2 receptor affinity and P-gp activity, suggesting that the absence of a hydrogen-bond donator at the thiosemicarbazone moiety reduces the interaction with the σ_2 and P-gp proteins, but it is not detrimental to the metal chelation property and to the overall antiproliferative effect. As a matter of fact, N-terminal dimethylation in the thiosemicarbazones structure has often resulted in enhanced antitumor activity, as demonstrated with the di-2-pyridyl (DpT),[38] and 2-benzoylpyridine (BpT)[46,47] thiosemicarbazones series. Di-2-pyridylketone-4,4-dimethyl-3-thiosemicarbazone (Dp44mT) belonging to the DpT series and 2-benzoylpyridine-4,4-dimethyl-3-thiosemicarbazone (Bp44mT) belonging to the BpT one emerged for their selective antitumor activity and were investigated in preclinical tumor models providing very promising results.[44,48] In addition, dimethylation of the terminal nitrogen importantly affected the activity of the analogs of the antitumor agent 3-aminopyridine-2-carboxaldehyde thiosemicarbazone (Triapine),[45] so that further studies were conducted to deepen the mode of action of these 2-pyridinecarbaldehyde thiosemicarbazones compared to the non-dimethylated counterparts.[49,50] However, in the multitarget agents herein presented, the overall effect is hardly predictable as shown by the compounds devoid of antiproliferative activity

despite their metal chelation properties and their activity at the σ_2 and P-gp proteins. One of the reasons is that σ_2-ligands may interact with σ_2 receptors as agonists (antiproliferative agents) or as antagonists (lack of antiproliferation), and there are no clear structural requirements that confer agonist *vs.* antagonist activity nor a well established *in vitro* assay to predict it. As already stated, small structural modifications in the structures of P-gp modulators are able to modify the interaction mechanism at the pump, transforming P-gp transported substrates into inhibitors (no ATP depletion). As for iron chelators that affect the cell red-ox equilibrium, activation of different cell death mechanisms (*e.g.* metal dependent radical damage, ribonucleotide reductase inhibitor, DNA binding, inhibition of protein synthesis) have been reported. In addition, contribution of off-targets effects to the overall activity of these compounds cannot be ruled out. That said, the multitarget strategy that was adopted produced several compounds with important antiproliferative activity in parent and resistant cells, with some differences between the two cell lines pairs that denote different sensitivity to the mechanisms activated by these ligands. Therefore, activated mechanisms need to be further investigated in diverse tumor cells in particular for the most promising thiosemicarbazones such as **7a** and **7b**. Compounds such as **8a**, **10a** and **17a** emerge for their potent nanomolar EC_{50} values at the P-gp efflux pump in line with the most potent P-gp reference modulators. Since these compounds do not lead to ATP cell depletion they appear as notable P-gp inhibitors rather than substrates, encouraging further studies for their possible exploitation as P-gp blockers. All in all, novel compounds holding promises for the treatment of resistant tumors were obtained, widening the availability of drugs and pathways to be studied to face MDR.

3. Experimental section

3.1. Chemistry

Both column chromatography and flash column chromatography were performed with 60 Å pore size silica gel as the stationary phase (1 : 30 w/w, 63–200 μm particle size, from ICN, and 1 : 15 w/w, 15–40 μm particle size, from Merck, respectively). Melting points were determined in open capillaries on a Gallenkamp electrothermal apparatus. Purity of tested compounds was established by high-performance liquid chromatography (HPLC) on an Agilent Infinity 1260 system equipped with diode array with a multiwavelength UV/vis detector set at λ = 230 nm, 254 nm and 280 nm, through a Phenomenex Gemini RP-18 column (250 × 4.6 mm, 5 μm particle size). ^{1}H NMR spectra were recorded on a Mercury Varian 300 MHz or on a 500-vnmrs500 Agilent spectrometer (499.801 MHz). The following data were reported: chemical shift (δ) in parts per million (ppm), multiplicity (s = singlet, d = doublet, t = triplet, m = multiplet), integration, and coupling constant(s) in hertz. For some representative compounds, heteronuclear single quantum coherence spectroscopy (2D-HSCQ) between ^{1}H and ^{13}C NMR spectra were recorded on a 500-vnmrs500 Agilent spectrometer (**11a**, **14a**) to assign signals, whereas NOESY 1D to ascertain the geometry of the double bond between the C- and N-atoms (**14a**). Recording of mass spectra was done on an Agilent 1100 series LCMSD trap system VL mass spectrometer; only significant *m*/*z* peaks, with their percentage of relative intensity in parentheses, are reported. High resolution mass spectroscopy (HRMS) was performed on a Agilent 6530 Accurate-Mass Q-TOF LC/MS spectrometer. Chemicals were from Aldrich, TCI and Alpha Aesar and were used without any further purification.

3.2. General procedure for the synthesis of 1-[4-(6,7-dimethoxy-3,4-dihydroisoquinolin-2(1*H*)-yl)butyl]indoline-2,3-dione hydrochloride (4a) and 1-(4-(4-cyclohexylpiperazin-1-yl)butyl)indoline-2,3-dione dihydrochloride (4b)

A solution of **3** (2.85 g, 12 mmol) in CH_3CN (30 mL) was added with K_2CO_3 (14 mmol, 1.94 g) and either 6,7-dimethoxy-1,2,3,4-tetrahydroisoquinoline or 1-cyclohexylpiperazine (14 mmol). The resulting mixture was refluxed overnight under stirring. After the removal of the solvent under reduced pressure the residue was taken up with H_2O and extracted with AcOEt (3 × 10 mL). The collected organic layers were dried (Na_2SO_4) and evaporated under reduced pressure to afford a crude oil which was purified by column chromatography (CH_2Cl_2/MeOH 95 : 5) to give the title compounds which were transformed into the corresponding hydrochloride salts.

3.2.1. 1-[4-(6,7-Dimethoxy-3,4-dihydroisoquinolin-2(1*H*)-yl)-butyl]indoline-2,3-dione hydrochloride (4a). 1-[4-(6,7-Dimethoxy-3,4-dihydroisoquinolin-2(1*H*)-yl)butyl]indoline-2,3-dione hydrochloride (**4a**) was obtained as orange crystals (2.36 g, 50% yield), mp = 134–136 °C; ^{1}H NMR (500 MHz, DMSO-d_6) δ 1.68–1.90 (m, 4H, CH_2CH_2CH_2N), 2.85–2.95 (m, 1H, NCH$_2$C*H*HAr), 3.17–3.32 (m, 4H, CH_2NCH_2CH_2Ar), 3.58–3.65 (m, 1H, NCH$_2$-CH*H*Ar), 3.71–3.79 (m, 8H, OCH$_3$ and CONCH$_2$), 4.10–4.23 (m, 1H, NC*H*HAr), 4.35–4.45 (m, 1H, NCH*H*Ar), 6.75 (s, 1H, aromatic), 6.80 (s, 1H, aromatic), 7.14 (t, 1H, J = 7.3 Hz, aromatic), 7.24 (d, 1H, J = 7.8 Hz, aromatic), 7.56 (d, 1H, J = 7.3 Hz, aromatic), 7.67 (t, 1H, J = 7.8 Hz, aromatic), 10.8 (broad s, 1H, NH); LC-MS (ESI$^+$) *m*/*z*: 417 [M + Na]$^+$; LC-MS-MS 417: 248, 179.

3.2.2. 1-(4-(4-Cyclohexylpiperazin-1-yl)butyl)indoline-2,3-dione dihydrochloride (4b). 1-(4-(4-Cyclohexylpiperazin-1-yl)butyl) indoline-2,3-dione dihydrochloride (**4b**) was obtained as orange crystals (2.1 g, 48% yield); mp = 250 °C dec.; ^{1}H-NMR (recorded on compound as free base; 300 MHz, $CDCl_3$) δ 1.06–1.89 (m, 14H, cyclohexyl CH$_2$ and CH_2CH_2CH_2N), 2.19–2.70 (m, 11H, piperazine CH and CH$_2$ and (CH$_2$)$_3$CH_2N), 3.73 (t, 2H, J = 7.3 Hz, NCH$_2$), 6.93 (d, 1H, J = 7.6 Hz, aromatic), 7.10 (t, 1H, J = 7.6 Hz, aromatic), 7.54–7.60 (m, 2H, aromatic); LC-MS (ESI$^+$) *m*/*z*: 370 [M + H]$^+$; LC-MS-MS 370: 288, 202.

3.3. General procedure for the synthesis of final thiosemicarbazones 5a,b–17a,b

To a solution of either **4a** or **4b** (0.57 mmol) in hot ethanol one among different thiosemicarbazides (0.57 mmol) was added. The mixture was refluxed for 4 h and upon cooling the precipitation of the final product was observed. The solid was filtered on a Gooch crucible and washed with cold EtOH. Purification through crystallization was achieved as reported for each compound.

3.3.1. (*Z*)-2-(1-(4-(6,7-Dimethoxy-3,4-dihydroisoquinolin-2(1*H*)-yl)butyl)-2-oxoindolin-3-ylidene)hydrazinecarbothioamide hydrochloride (5a). Crystallization from H_2O/EtOH afforded the title compound as yellow solid (0.049 g, 17% yield), mp = 237 °C (dec.); ^{1}H-NMR (500 MHz, DMSO-d_6) δ 1.71–1.81 (m, 4H, CH_2-CH_2CH$_2$N), 2.88–2.91 (m, 1H, NCH$_2$C*H*HAr), 3.09–3.25 (m, 4H, CH_2NCH_2CH$_2$Ar), 3.56–3.64 (m, 1H, NCH$_2$CH*H*Ar), 3.71 (s, 3H, OCH$_3$), 3.72 (s, 3H, OCH$_3$), 3.79–3.81 (m, 2H, CONCH$_2$), 4.14–4.18 (m, 1H, NC*H*HAr), 4.31–4.37 (m, 1H, NC*H*HAr), 6.76 (s, 1H, aromatic), 6.79 (s, 1H, aromatic), 7.15–7.18 (m, 1H, aromatic), 7.22–7.24 (m, 1H, aromatic), 7.42–7.45 (m, 1H, aromatic), 7.71–7.73 (m, 1H, aromatic), 8.75 (s, 1H, NH), 9.09 (s, 1H, NH), 10.57 (broad s, 1H, NH), 12.41 (s, 1H, NH). Compound was >98% pure by HPLC analysis performed with CH$_3$CN/H$_2$O/HCOONH$_4$ (20 mM, pH = 5), 75 : 25 v/v, at a flow rate 1 mL min^{-1}.

3.3.2. (*Z*)-2-[1-[4-(4-Cyclohexylpiperazin-1-yl)butyl]-2-oxoindolin-3-ylidene]hydrazinecarbothioamide dihydrochloride (5b). Crystallization from H_2O/MeOH afforded the title compound as a yellow solid, (0.102 g, yield 35%); mp = 250 °C (dec.); ^{1}H-NMR (500 MHz, DMSO-d_6) δ 1.05–2.20 (m, 14H, cyclohexyl CH$_2$ and CH_2CH_2CH$_2$N), 3.10–3.90 (m, 13H, NCH$_2$, CONCH$_2$ and cyclohexyl CH), 7.13–7.17 (m, 1H, aromatic), 7.22–7.24 (m, 1H, aromatic), 7.42–7.46 (m, 1H, aromatic), 7.73–7.75 (m, 1H, aromatic), 8.16 (s, 1H, NH), 11.60–12.00 (broad s, 2H, NH), 12.47 (s, 1H, NH). Compound was >98% pure by HPLC analysis performed with CH$_3$CN/H$_2$O/HCOONH$_4$ (20 mM, pH = 5), 75 : 25 v/v, at a flow rate 1 mL min^{-1}.

3.3.3. (*Z*)-2-(1-(4-(6,7-Dimethoxy-3,4-dihydroisoquinolin-2(1*H*)-yl)butyl)-2-oxoindolin-3-ylidene)-*N*-methylhydrazinecarbothioamide hydrochloride (6a). Crystallization from H_2O/MeOH afforded the title compound as yellow powder (0.188 g, 64% yield), mp = 224–226 °C; ^{1}H NMR (500 MHz, DMSO-d_6) δ 1.69–1.88 (m, 4H, CH_2CH_2CH$_2$N), 2.85–2.93 (m, 1H, NCH$_2$-C*H*HAr), 3.09 (d, 3H, J = 4.4 Hz, CH$_3$), 3.15–3.28 (m, 4H, CH_2-NCH_2CH$_2$Ar), 3.53–3.65 (m, 1H, NCH$_2$CH*H*Ar), 3.71 (s, 3H, OCH$_3$), 3.73 (s, 3H, OCH$_3$), 3.81 (t, 2H, J = 6.8 Hz, CONCH$_2$), 4.08–4.17 (m, 1H, NC*H*HAr), 4.32–4.39 (m, 1H, NCH*H*Ar), 6.78 (s, 1H, aromatic), 6.80 (s, 1H, aromatic), 7.16–7.19 (m, 1H, aromatic), 7.24 (d, 1H, J = 7.8 Hz, aromatic), 7.45 (t, 1H, J = 7.8 Hz, aromatic), 7.71 (d, 1H, J = 7.3 Hz, aromatic), 9.33 (q, 1H, J = 4.4 Hz, N*H*CH$_3$), 10.7 (br s, 1H, NH, D$_2$O exchanged), 12.53 (s, 1H, NH); LC-MS (ESI$^+$) m/z: 482 [M + H]$^+$; 504 [M + Na]$^+$; LC-MS-MS 482: 451, 365; LC-MS (ESI$^-$) m/z 480 [M − H]$^-$; LC-MS-MS 480: 407, 379; HRMS calculated for $C_{25}H_{31}N_5O_3S$ 482.2220 [M + H]$^+$, found 482.2219. Compound was >98% pure by HPLC analysis performed either with CH$_3$CN/H$_2$O/HCOONH$_4$ (20 mM, pH = 5), 75 : 25 v/v at a flow rate 1 mL min^{-1} or with MeOH/H$_2$O, 82 : 18 at a flow rate 0.8 mL min^{-1}.

3.3.4. (*Z*)-2-[1-[4-(4-Cyclohexylpiperazin-1-yl)butyl]-2-oxoindolin-3-ylidene]-*N*-methylhydrazinecarbothioamide di-hydrochloride (6b). Crystallization from H_2O/MeOH afforded the title compound as a yellow solid; mp = 250 °C (dec.) (0.186 g, yield 62%); ^{1}H-NMR (500 MHz, CD$_3$OD + D$_2$O) δ 1.17–2.18 (m, 14H, cyclohexyl CH$_2$ and CH_2CH_2CH$_2$N), 3.20 (s, 3H, NCH$_3$), 3.27–3.80 (m, 11H, CHN and CH$_2$N), 3.88–3.98 (m, 2H, CONCH$_2$), 7.13–7.19 (m, 2H, aromatic), 7.45 (t, 1H, J = 7.8, aromatic), 7.74 (d, 1H, J = 7.8, aromatic); LC-MS (ESI$^+$) m/z: 457 [M + H]$^+$; LC-MS-MS 457: 426, 340; LC-MS (ESI$^-$): 455 [M − H]$^-$; LC-MS-MS 455: 382. HRMS calculated for $C_{24}H_{36}N_6OS$ 457.2744 [M + H]$^+$, found 457.2744. Compound was >98% pure by HPLC analysis performed either with CH$_3$CN/H$_2$O/HCOONH$_4$ (20 mM, pH = 5), 75 : 25 v/v or with MeOH/H$_2$O, 80 : 20 at a flow rate 1 mL min^{-1}.

3.3.5. (*Z*)-2-(1-(4-(6,7-Dimethoxy-3,4-dihydroisoquinolin-2(1*H*)-yl)butyl)-2-oxoindolin-3-ylidene)-*N*,*N*-dimethylhydrazinecarbothioamide hydrochloride (7a). Crystallization from H_2O/MeOH afforded the title compound as yellow powder, mp = 194–196 °C; ^{1}H NMR (500 MHz, DMSO-d_6) δ 1.72–1.82 (m, 4H, CH_2-CH_2CH$_2$N), 2.81–2.97 (m, 1H, NCH$_2$C*H*HAr), 3.18–3.25 (m, 4H, CH_2NCH_2CH$_2$Ar), 3.39 (s, 6H, N(CH$_3$)$_2$), 3.58–3.64 (m, 1H, NCH$_2$CH*H*Ar), 3.70 (s, 3H, OCH$_3$), 3.74 (s, 3H, OCH$_3$), 3.83 (t, 2H, J = 6.6 Hz, CONCH$_2$), 4.01–4.18 (m, 1H, NC*H*HAr), 4.35–4.40 (m, 1H, NCH*H*Ar), 6.76 (s, 1H, aromatic), 6.80 (s, 1H, aromatic), 7.17 (t, 1H, J = 7.3 Hz, aromatic), 7.26 (d, 1H, J = 7.8 Hz, aromatic), 7.45 (t, 1H, J = 7.8 Hz, aromatic), 7.60 (d, 1H, J = 7.3 Hz, aromatic), 10.7 (broad s, 1H, NH), 13.38 (s, 1H, NH); LC-MS (ESI$^+$) m/z 518 [M + Na]$^+$; LC-MS-MS 518: 473, 415; LC-MS (ESI$^-$) m/z 494 [M − H]$^-$; LC-MS-MS 494: 466, 233. Compound was >98% pure by HPLC analysis performed with CH$_3$CN/H$_2$O/HCOONH$_4$ (20 mM, pH = 5), 75 : 25 v/v at a flow rate 1 mL min^{-1}.

3.3.6. (*Z*)-2-[1-[4-(4-Cyclohexylpiperazin-1-yl)butyl]-2-oxoindolin-3-ylidene]-*N*,*N*-dimethylhydrazinecarbothioamide di-hydrochloride (7b). Crystallization from H_2O/MeOH afforded the title compound as yellow powder (0.173 g, yield 56%), mp = 250 °C (dec.); ^{1}H-NMR (500 Hz, CD$_3$OD + D$_2$O) δ 1.16–2.20 (m, 14H, cyclohexyl CH$_2$ and CH_2CH_2CH$_2$N), 3.24–3.28 (m, 2H, NCH$_2$), 3.30–3.34 (m, 6H, N(CH$_3$)$_2$), 3.38–3.80 (m, 9H, piperazine CH$_2$ and cyclohexyl CH), 3.86–3.92 (m, 2H, CONCH$_2$), 7.13–7.18 (m, 1H, aromatic), 7.19–7.24 (m, 1H, aromatic), 7.44–7.50 (m, 1H, aromatic), 7.86–7.90 (m, 1H, aromatic); LC-MS (ESI$^+$): m/z 471 [M + H]$^+$; LC-MS-MS 471: 426; LC-MS (ESI$^-$): m/z 469 [M − H]$^-$; LC-MS-MS 469: 441, 385. HRMS calculated for $C_{25}H_{38}N_6OS$ 471.289 [M + H]$^+$, found 471.2901. Compound was >98% pure by HPLC analysis performed with CH$_3$CN/H$_2$O/HCOONH$_4$ (20 mM, pH = 5), 75 : 25 v/v at a flow rate 1 mL min^{-1}.

3.3.7. (*Z*)-2-(1-(4-(6,7-Dimethoxy-3,4-dihydroisoquinolin-2(1*H*)-yl)butyl)-2-oxoindolin-3-ylidene)-*N*-i-propylhydrazinecarbothioamide hydrochloride (8a). Crystallization from H_2O/EtOH afforded the title compound as a yellow solid, (0.204 g, yield 65%); mp = 189 °C (dec.); ^{1}H-NMR (500 MHz, DMSO-d_6) δ 1.26 (d, 6H, J = 6.36 Hz, CH(CH_3)$_2$), 1.69–1.90 (m, 4H, CH_2CH_2CH$_2$N), 2.88–2.96 (m, 1H, NCH$_2$C*H*HAr), 3.05–3.30 (m, 4H, CH_2NCH_2CH$_2$Ar), 3.60–3.68 (m, 1H, NCH$_2$CH*H*Ar), 3.70 (s, 3H, OCH$_3$), 3.74 (s, 3H, OCH$_3$), 3.84 (t, 2H, J = 6.85 Hz, CONCH$_2$), 4.10–4.19 (m, 1H, NC*H*HAr), 4.33–4.40 (m, 1H, NCH*H*Ar), 4.49–4.58 (m, 1H, C*H*(CH$_3$)$_2$), 6.77 (s, 1H, aromatic), 6.80 (s, 1H, aromatic), 7.16–7.19 (m, 1H, aromatic), 7.23 (d, 1H, J = 7.83 Hz, aromatic), 7.43–7.46 (m, 1H, aromatic), 7.79–7.81 (m, 1H, aromatic), 8.94 (d, 1H, J = 8.80 Hz, NH), 10.62 (broad s, 1H, NH), 12.52 (s, 1H, NH); LC-MS (ESI$^+$) m/z: 510 [M + H]$^+$; 532 [M + Na]$^+$; LC-MS-MS 532: 473. Compound was >98% pure by HPLC analysis performed with

$CH_3CN/H_2O/HCOONH_4$ (20 mM, pH = 5), 75 : 25 v/v, at a flow rate 1 mL min^{-1}.

3.3.8. (*Z*)-2-[1-[4-(4-Cyclohexylpiperazin-1-yl)butyl]-2-oxoindolin-3-ylidene]-*N*-i-propylhydrazinecarbothioamide dihydrochloride (8b). Crystallization from H_2O/MeOH afforded the title compound as a yellow solid, (0.167 g, yield 53%); mp = 250 °C (dec.); ^{1}H-NMR (500 MHz, DMSO-d_6) δ 1.05–2.20 (m, 20H, cyclohexyl CH_2, $CH(CH_3)_2$ and $CH_2CH_2CH_2N$), 3.20–3.85 (m, 13H, NCH_2, $CONCH_2$ and cyclohexyl CH), 4.49–4.56 (m, 1H, $CH(CH_3)_2$), 7.15–7.18 (m, 1H, aromatic), 7.21–7.24 (m, 1H, aromatic), 7.42–7.45 (m, 1H, aromatic), 7.78–7.80 (m, 1H, aromatic), 8.91–8.93 (m, 1H, NH), 11.50–12.00 (broad s, 2H, NH), 12.49 (s, 1H, NH); LC-MS (ESI^+): *m*/*z* 485 $[M + H]^+$; LC-MS-MS 485: 426. LC-MS (ESI^-): *m*/*z* 483 $[M - H]^-$; LC-MS-MS 483: 382. Compound was >98% pure by HPLC analysis performed with $CH_3CN/H_2O/HCOONH_4$ (20 mM, pH = 5), 75 : 25 v/v, at a flow rate 1 mL min^{-1}.

3.3.9. (*Z*)-2-(1-(4-(6,7-Dimethoxy-3,4-dihydroisoquinolin-2(1*H*)-yl)butyl)-2-oxoindolin-3-ylidene)-*N*-(*tert*-butyl)hydrazinecarbothioamide hydrochloride (9a). Crystallization from EtOH/H_2O afforded the title compound as yellow solid (0.053 g, 16% yield), mp = 206 °C (dec.); ^{1}H-NMR (500 MHz, DMSO-d_6) δ 1.56 (s, 9H, $C(CH_3)_3$), 1.69–1.81 (m, 4H, $CH_2CH_2CH_2N$), 2.87–2.91 (m, 1H, NCH_2CHHAr), 3.12–3.28 (m, 4H, $CH_2NCH_2CH_2Ar$), 3.58–3.62 (m, 1H, NCH_2CHHAr), 3.71 (s, 3H, OCH_3), 3.73 (s, 3H, OCH_3), 3.80–3.82 (m, 2H, $CONCH_2$), 4.10–4.15 (m, 1H, $NCHHAr$), 4.35–4.40 (m, 1H, $NCHHAr$), 6.76 (s, 1H, aromatic), 6.80 (s, 1H, aromatic), 7.14–7.17 (m, 1H, aromatic), 7.23–7.25 (m, 1H, aromatic), 7.43–7.46 (m, 1H, aromatic), 7.75–7.76 (m, 1H, aromatic), 8.16 (s, 1H, NH), 10.56 (broad s, 1H, NH), 12.50 (s, 1H, NH); LC-MS (ESI^+) *m*/*z*: 524 $[M + H]^+$; 546 $[M + Na]^+$; LC-MS-MS 524: 451; LC-MS (ESI^-) *m*/*z* 522 $[M - H]^-$; LC-MS-MS 522: 407. Compound was >98% pure by HPLC analysis performed with $CH_3CN/H_2O/HCOONH_4$ (20 mM, pH = 5), 75 : 25 v/v, at a flow rate 1 mL min^{-1}.

3.3.10. (*Z*)-*N*-*t*-Butyl-2-[1-[4-(4-cyclohexylpiperazin-1-il)butyl]-2-oxoindolin-3-ylidene]hydrazinecarbothioamidehydrochloride (9b). Crystallization from H_2O/MeOH afforded the title compound as yellow solid (0.175 g, 54% yield), mp = 250 °C (dec.); ^{1}H-NMR (500 MHz, DMSO-d_6): δ 1.08–2.20 (m + s, 23H, 14H, cyclohexyl CH_2, $C(CH_3)_3$ and $CH_2CH_2CH_2N$), 3.10–3.82 (m, 13H, NCH_2, $CONCH_2$ and cyclohexyl CH), 7.13–7.17 (m, 1H, aromatic), 7.22–7.24 (m, 1H, aromatic), 7.42–7.46 (m, 1H, aromatic), 7.73–7.75 (m, 1H, aromatic), 8.16 (s, 1H, NH), 11.60–12.00 (broad s, 2H, NH), 12.47 (s, 1H, NH); LC-MS (ESI^+) *m*/*z* 499 $[M + H]^+$; LC-MS-MS 499: 426. LC-MS (ESI^-): *m*/*z* 497 $[M - H]^-$; LC-MS-MS 497: 382. Compound was >98% pure by HPLC analysis performed with $CH_3CN/H_2O/HCOONH_4$ (20 mM, pH = 5), 75 : 25 v/v, at a flow rate 1 mL min^{-1}.

3.3.11. (*Z*)-2-(1-(4-(6,7-Dimethoxy-3,4-dihydroisoquinolin-2(1*H*)-yl)butyl)-2-oxoindolin-3-ylidene)-*N*-benzylhydrazinecarbothioamide hydrochloride (10a). Trituration with H_2O/MeOH (1/1) followed by washing with MeOH afforded the title compound as yellow solid (0.224 g, 65% yield), mp = 240 °C (dec.); ^{1}H-NMR (500 MHz, DMSO-d_6) δ 1.69–1.90 (m, 4H, $CH_2CH_2CH_2N$), 2.86–2.93 (m, 1H, NCH_2CHHAr), 3.04–3.28 (m, 4H, $CH_2NCH_2CH_2Ar$), 3.59–3.67 (m, 1H, NCH_2CHHAr), 3.71 (s, 3H, OCH_3), 3.73 (s, 3H, OCH_3), 3.82 (t, 2H, *J* = 6.85 Hz, $CONCH_2$), 4.10–4.19 (m, 1H, $NCHHAr$), 4.35–4.41 (m, 1H, $NCHHAr$), 4.88–4.90 (m, 2H, benzyl CH_2), 6.77 (s, 1H, aromatic), 6.80 (s, 1H, aromatic), 7.18–7.21 (m, 1H, aromatic), 7.22–7.29 (m, 2H, aromatic), 7.31–7.40 (m, 4H, aromatic), 7.42–7.47 (m, 1H, aromatic), 7.84–7.86 (m, 1H, aromatic), 9.78–9.98 (m, 1H, NH), 10.66 (broad s, 1H, NH), 12.70 (s, 1H, NH); LC-MS (ESI^+) *m*/*z*: 558 $[M + H]^+$; 580 $[M + Na]^+$; LC-MS-MS 558: 451. Compound was >98% pure by HPLC analysis performed with $CH_3CN/H_2O/HCOONH_4$ (20 mM, pH = 5), 75 : 25 v/v, at a flow rate 1 mL min^{-1}.

3.3.12. (*Z*)-*N*-Benzyl-2-[1-[4-(4-cyclohexylpiperazin-1-yl)-butyl]-2-oxoindolin-3-ylidene]hydrazinecarbothioamide dihydrochloride (10b). Crystallization from H_2O/MeOH afforded the title compound as yellow solid (0.235 g, 69% yield), mp = 250 °C (dec.); ^{1}H-NMR (500 MHz, DMSO-d_6) δ 1.05–2.20 (m, 14H, cyclohexyl CH_2 and $CH_2CH_2CH_2N$), 3.10–3.85 (m, 13H, NCH_2, $CONCH_2$ and cyclohexyl CH), 4.85–4.95 (m, 2H, benzyl CH_2), 7.15–7.20 (m, 1H, aromatic), 7.20–7.30 (m, 2H, aromatic), 7.31–7.40 (m, 4H, aromatic), 7.40–7.50 (m, 1H, aromatic), 7.70–7.75 (m, 1H, aromatic), 9.85–9.92 (m, 1H, NH); 11.14–11.85 (broad s, 2H, NH); 12.52–12.66 (m, 1H, NH). Compound was >98% pure by HPLC analysis performed with $CH_3CN/H_2O/HCOONH_4$ (20 mM, pH = 5), 75 : 25 v/v, at a flow rate 1 mL min^{-1}.

3.3.13. (*Z*)-2-(1-(4-(6,7-Dimethoxy-3,4-dihydroisoquinolin-2(1*H*)-yl)butyl)-2-oxoindolin-3-ylidene)-*N*-phenylhydrazinecarbothioamide hydrochloride (11a). Trituration from MeOH afforded the title compound as orange powder (0.151 g, 48% yield), mp = 212 °C (dec.); ^{1}H NMR (500 MHz, DMSO-d_6) δ 1.73–1.84 (m, 4H, $CH_2CH_2CH_2N$), 2.90–3.11 (m, 1H, NCH_2CHHAr), 3.16–3.26 (m, 4H, $CH_2NCH_2CH_2Ar$), 3.58–3.64 (m, 1H, NCH_2-$CHHAr$), 3.71 (s, 3H, OCH_3), 3.73 (s, 3H, OCH_3), 3.83 (t, 2H, *J* = 6.8 Hz, $CONCH_2$), 4.01–4.18 (m, 1H, $NCHHAr$), 4.35–4.40 (m, 1H, $NCHHAr$), 6.76 (s, 1H, aromatic), 6.8 (s, 1H, aromatic), 7.17–7.21 (m, 1H, aromatic), 7.25–7.30 (m, 2H, aromatic), 7.41–7.49 (m, 3H, aromatic), 7.59–7.62 (m, 2H, aromatic), 7.86 (d, 1H, *J* = 6.8 Hz, aromatic), 10.80 (broad s, 1H, NH), 10.90 (s, 1H, NHAr), 12.74 (s, 1H, NHCS); HSQC (^1H–^{13}C) signals are in agreement with the reported assignments. LC-MS (ESI^+) *m*/*z*: 544 $[M + H]^+$; 566 $[M + Na]^+$; LC-MS-MS 544: 451, 365; LC-MS (ESI^-) *m*/*z* 542 $[M - H]^-$; LC-MS-MS 542: 407; HRMS calculated for $C_{30}H_{33}N_5O_3S$ $[M + H]^+$ 544.2377, found 544.2378. Compound was >98% pure by HPLC analysis performed with $CH_3CN/H_2O/HCOONH_4$ (20 mM, pH = 5), 75 : 25 v/v or with MeOH/H_2O 80 : 20 v/v, at a flow rate 1 mL min^{-1}.

3.3.14. (*Z*)-2-[1-[4-(4-Cyclohexylpiperazin-1-yl)butyl]-2-oxoindolin-3-yliden]-*N*-phenylhydrazinecarbothioamide di-hydrochloride (11b). Crystallization from H_2O/MeOH afforded the title compound as yellow powder (0.180 g, yield 54%), mp = 250 °C (dec.); ^{1}H-NMR (500 Hz, CD_3OD + D_2O) δ 1.20–2.20 (m, 14H, cyclohexyl CH_2 and $CH_2CH_2CH_2N$), 3.24–3.28 (m, 2H, NCH_2), 3.20–3.95 (m, 13H, NCH_2, $CONCH_2$ and cyclohexyl CH), 7.10–7.16 (m, 1H, aromatic), 7.17–7.27 (m, 1H, aromatic), 7.30–7.36 (m, 1H, aromatic), 7.39–7.51 (m, 3H, aromatic), 7.51–7.59 (m, 2H, aromatic); LC-MS (ESI^+): *m*/*z* 519 $[M + H]^+$; LC-MS-MS 519: 426, 340; LC-MS (ESI^-): *m*/*z* 517 $[M - H]^-$; LC-MS-MS 517: 382. HRMS calculated for $C_{29}H_{38}N_6OS$ 519.2901 $[M + H]^+$, found 519.2899. Compound was >98% pure by HPLC analysis

performed with $CH_3CN/H_2O/HCOONH_4$ (20 mM, pH = 5), 75 : 25 v/v at a flow rate 1 mL min^{-1}.

3.3.15. (*Z*)-2-(1-(4-(6,7-Dimethoxy-3,4-dihydroisoquinolin-2(1*H*)-yl)butyl)-2-oxoindolin-3-ylidene)-*N*-(*p*-tolyl)hydrazinecarbothioamide hydrochloride (12a). Crystallization from H_2O/EtOH afforded the title compound as orange powder (0.157 g, 45% yield), mp = 164 °C dec.; ^{1}H NMR (500 MHz, DMSO-d_6) δ 1.71–1.88 (m, 4H, CH_2CH_2CH_2N), 2.33 (s, 1H, PhCH_3), 2.87–2.95 (m, 1H, NCH_2C*H*HAr), 3.06–3.27 (m, 4H, CH_2NCH_2CH_2Ar), 3.57–3.66 (m, 1H, NCH_2CH*H*Ar), 3.71 (s, 3H, OCH_3), 3.73 (s, 3H, OCH_3), 3.83 (t, 2H, J = 6.8 Hz, CONCH_2), 4.10–4.19 (m, 1H, NC*H*HAr), 4.33–4.40 (m, 1H, NCH*H*Ar), 6.76 (s, 1H, aromatic), 6.8 (s, 1H, aromatic), 7.18–7.23 (m, 4H, aromatic), 7.43–7.48 (m, 3H, aromatic), 7.82–7.87 (m, 1H, aromatic), 10.63 (broad s, 1H, NH), 10.92 (s, 1H, NHAr), 12.76 (s, 1H, NH); LC-MS (ESI$^+$) m/z: 558 [M + H]$^+$; 580 [M + Na]$^+$; LC-MS-MS 558: 451, 365; 580: 473, 415; LC-MS (ESI$^-$) m/z 556 [M − H]$^-$; LC-MS-MS 556: 407. Compound was >98% pure by HPLC analysis performed with $CH_3CN/H_2O/HCOONH_4$ (20 mM, pH = 5), 75 : 25 v/v, at a flow rate 1 mL min^{-1}.

3.3.16. (*Z*)-2-[1-[4-(4-Cyclohexylpiperazin-1-yl)butyl]-2-oxoindolin-3-yliden]-*N*-(4-metilphenyl)hydrazinecarbothioamide dihydrochloride (12b). Crystallization from H_2O/MeOH afforded the title compound as yellow powder (0.240 g, yield 70%), mp = 250 °C (dec.); ^{1}H-NMR (500 MHz, DMSO-d_6 + D_2O) δ 1.00–2.04 (m, 14H, cyclohexyl CH_2 and CH_2CH_2CH_2N), 2.28 (s, 3H, PhCH_3), 3.08–3.90 (m, 13H, NCH_2, CONCH_2 and cyclohexyl CH), 7.13–7.18 (m, 2H, aromatic), 7.18–7.22 (m, 2H, aromatic), 7.36–7.41 (m, 2H, aromatic), 7.42–7.47 (m, 1H, aromatic), 7.77–7.81 (m, 1H, aromatic); LC-MS (ESI$^+$): m/z 533 [M + H]$^+$; LC-MS-MS 533: 426; LC-MS (ESI$^-$): m/z 531 [M − H]$^-$; LC-MS-MS 531: 382. Compound was >98% pure by HPLC analysis performed with $CH_3CN/H_2O/HCOONH_4$ (20 mM, pH = 5), 75 : 25 v/v, at a flow rate 1 mL min^{-1}.

3.3.17. (*Z*)-2-(1-(4-(6,7-Dimethoxy-3,4-dihydroisoquinolin-2(1*H*)-yl)butyl)-2-oxoindolin-3-ylidene)-*N*-(4-methoxyphenyl)-hydrazinecarbothioamide hydrochloride (13a). Crystallization from EtOH afforded the title compound as orange solid (0.170 g, 49% yield), mp = 152 °C (dec.); ^{1}H-NMR (500 MHz, DMSO-d_6) δ 1.72–1.83 (m, 4H, CH_2CH_2CH_2N), 2.88–2.91 (m, 1H, NCH_2-C*H*HAr), 3.10–3.28 (m, 4H, CH_2NCH_2CH_2Ar), 3.60–3.63 (m, 1H, NCH_2CH*H*Ar), 3.71 (s, 3H, OCH_3), 3.72 (s, 3H, OCH_3), 3.78 (s, 3H, OCH_3), 3.83 (t, 2H, J = 6.36 Hz, CONCH_2), 4.12–4.15 (m, 1H, NC*H*HAr), 4.35–4.38 (m, 1H, NCH*H*Ar), 6.77 (s, 1H, aromatic), 6.80 (s, 1H, aromatic), 6.97–6.99 (m, 2H, aromatic), 7.17–7.20 (m, 1H, aromatic), 7.25–7.26 (m, 1H, aromatic), 7.43–7.47 (m, 3H, aromatic), 7.83–7.85 (m, 1H, aromatic), 10.57 (broad s, 1H, NH), 10.80 (s, 1H, NHAr), 12.69 (s, 1H, NH); LC-MS (ESI$^+$) m/z: 574 [M + H]$^+$; 596 [M + Na]$^+$; LC-MS-MS 574: 451; LC-MS (ESI$^-$) m/z 572 [M − H]$^-$; LC-MS-MS 572: 407. Compound was >98% pure by HPLC analysis performed with $CH_3CN/H_2O/HCOONH_4$ (20 mM, pH = 5), 75 : 25 v/v, at a flow rate 1 mL min^{-1}.

3.3.18. (*Z*)-2-[1-[4-(4-Cyclohexylpiperazin-1-yl)butyl]-2-oxoindolin-3-ylidene]-*N*-(4-methoxyphenyl)hydrazinecarbothioamide hydrochloride (13b). Crystallization from H_2O/MeOH afforded the title compound as a yellow solid, (0.203 g, yield 61%); mp = 250 °C (dec.); ^{1}H-NMR (300 MHz, DMSO-d_6) δ 1.10–2.20 (m, 14H, cyclohexyl CH_2 and CH_2CH_2CH_2N), 3.00–3.85 (m, 13H, NCH_2, CONCH_2 and cyclohexyl CH), 3.78 (s, 3H, OCH_3), 6.90–7.00 (m, 2H, aromatic), 7.15–7.30 (m, 2H, aromatic), 7.40–7.55 (m, 3H, aromatic), 7.80–7.90 (m, 1H, aromatic), 10.80 (s, 1H, NH), 11.25–11.93 (broad s, 2H, NH), 12.66 (s, 1H, NH); LC-MS (ESI$^+$): m/z 549 [M + H]$^+$; LC-MS-MS 549: 426. LC-MS (ESI$^-$): m/z 547 [M − H]$^-$; LC-MS-MS 547: 382. Compound was >98% pure by HPLC analysis performed with $CH_3CN/H_2O/HCOONH_4$ (20 mM, pH = 5), 75 : 25 v/v, at a flow rate 1 mL min^{-1}.

3.3.19. (*Z*)-2-(1-(4-(6,7-Dimethoxy-3,4-dihydroisoquinolin-2(1*H*)-yl)butyl)-2-oxoindolin-3-ylidene)-*N*-(4-fluorophenyl)-hydrazinecarbothioamide hydrochloride (14a). Crystallization from H_2O/MeOH afforded the title compound as orange powder (0.170 g, 49% yield), mp = 163 °C; ^{1}H-NMR (500 MHz, DMSO-d_6) δ 1.73–1.83 (m, 4H, CH_2CH_2CH_2N), 2.85–2.91 (m, 1H, NCH_2-C*H*HAr), 3.10–3.31 (m, 4H, CH_2NCH_2CH_2Ar), 3.57–3.66 (m, 1H, NCH_2CH*H*Ar), 3.70 (s, 3H, OCH_3), 3.73 (s, 3H, OCH_3), 3.68–3.75 (m, 2H, CONCH_2), 4.07–4.18 (m, 1H, NC*H*HAr), 4.30–4.40 (m, 1H, NC*H*HAr), 6.75 (s, 1H, aromatic), 6.78 (s, 1H, aromatic), 7.18–7.28 (m, 4H, aromatic), 7.43–7.60 (m, 3H, aromatic), 7.81–7.83 (m, 1H, aromatic), 10.71 (broad s, 1H, NH), 10.89 (s, 1H, NHAr), 12.74 (s, 1H, NHCS); HSQC (^{1}H–^{13}C) signals are in agreement with the reported assignments and NOESY 1D with the reported geometry. LC-MS (ESI$^+$) m/z: 562 [M + H]$^+$; 584 [M + Na]$^+$; LC-MS-MS 562: 451; LC-MS-MS 584: 473; LC-MS (ESI$^-$) m/z 560 [M − H]$^-$; LC-MS-MS 556: 407. Compound was >98% pure by HPLC analysis performed with $CH_3CN/H_2O/HCOONH_4$ (20 mM, pH = 5), 75 : 25 v/v, at a flow rate 1 mL min^{-1}.

3.3.20. (*Z*)-2-[1-[4-(4-Cyclohexylpiperazin-1-yl)butyl]-2-oxoindolin-3-yliden]-*N*-(4-fluorophenyl)hydrazinecarbothioamide di-hydrochloride (14b). Crystallization from H_2O/MeOH afforded the title compound as yellow solid (0.145 g, resa 42%), mp = 250 °C (dec.); ^{1}H-NMR (500 MHz, DMSO-d_6) δ 1.00–2.04 (m, 14H, cyclohexyl CH_2 and CH_2CH_2CH_2N), 3.15–3.90 (m, 13H, NCH_2, CONCH_2 and cyclohexyl CH), 7.17–7.22 (m, 1H, aromatic), 7.24–7.28 (m, 2H, aromatic), 7.28–7.30 (m, 1H, aromatic), 7.44–7.50 (m, 1H, aromatic), 7.57–7.63 (m, 2H, aromatic); 7.81–7.85 (m, 1H, aromatic), 10.80–10.95 (m, 1H, NH, D_2O exchanged), 11.22–11.99 (broad s, 2H, NH piperazinium), 12.65–12.81 (m, 1H, NH, D_2O exchanged); LC-MS (ESI$^+$): m/z 537 [M + H]$^+$; LC-MS-MS 537: 426; LC-MS (ESI$^-$): m/z 535 [M − H]$^-$; LC-MS-MS 535: 382. Compound was >98% pure by HPLC analysis performed with $CH_3CN/H_2O/HCOONH_4$ (20 mM, pH = 5), 75 : 25 v/v, at a flow rate 1 mL min^{-1}.

3.3.21. (*Z*)-2-(1-(4-(6,7-Dimethoxy-3,4-dihydroisoquinolin-2(1*H*)-yl)butyl)-2-oxoindolin-3-ylidene)-*N*-(4-chlorophenyl)-hydrazinecarbothioamide hydrochloride (15a). Crystallization from H_2O/MeOH afforded the title compound as orange powder (0.170 g, 47% yield), mp = 172 °C (dec.); ^{1}H-NMR (500 MHz, DMSO-d_6) δ 1.71–1.90 (m, 4H, CH_2CH_2CH_2N), 2.86–2.94 (m, 1H, NCH_2C*H*HAr), 3.06–3.27 (m, 4H, CH_2NCH_2CH_2Ar), 3.58–3.67 (m, 1H, NCH_2CH*H*Ar), 3.71 (s, 3H, OCH_3), 3.73 (s, 3H, OCH_3), 3.83 (t, 2H, J = 6.85 Hz, CONCH_2), 4.10–4.19 (m, 1H, NC*H*HAr), 4.33–4.40 (m, 1H, NC*H*HAr), 6.77 (s, 1H, aromatic), 6.80 (s, 1H, aromatic), 7.18–7.21 (m, 1H, aromatic), 7.25–7.28 (m, 1H, aromatic), 7.47–7.51 (m, 3H, aromatic), 7.64–7.68 (m, 2H, aromatic), 7.84–7.86 (m, 1H, aromatic), 10.66 (broad s, 1H, NH), 10.93 (s, 1H, NHAr), 12.79 (s, 1H, NHCS); LC-MS (ESI$^+$) m/z: 578

$[M + H]^+$; 600 $[M + Na]^+$; LC-MS-MS 578: 451; LC-MS-MS 600: 473, 415. Compound was >98% pure by HPLC analysis performed with $CH_3CN/H_2O/HCOONH_4$ (20 mM, pH = 5), 75 : 25 v/v, at a flow rate 1 mL min^{-1}.

3.3.22. (*Z*)-*N*-(4-Chlorophenyl)-2-[1-[4-(4-cyclohexylpiperazin-1-yl)butyl]-2-oxoindolin-3-ylidene]hydrazinecarbothioamide dihydrochloride (15b). Crystallization from H_2O/MeOH afforded the title compound as yellow solid (0.220 g, 63% yield), mp = 250 °C (dec.); ^{1}H-NMR (500 MHz, DMSO-d_6) δ 1.00–2.24 (m, 14H, cyclohexyl CH_2 and CH_2CH_2CH_2N), 3.20–3.90 (m, 13H, NCH_2, $CONCH_2$ and cyclohexyl CH), 7.13–7.18 (m, 2H, aromatic), 7.18–7.22 (m, 2H, aromatic), 7.36–7.41 (m, 2H, aromatic), 7.42–7.47 (m, 1H, aromatic), 7.77–7.81 (m, 1H, aromatic), 10.75–11.01 (m, 1H, NH), 11.37–12.20 (broad s, 2H, NH); 12.73–12.99 (m, 1H, NH); LC-MS (ESI^+): *m*/*z* 553 $[M + H]^+$; LC-MS-MS 553: 426. Compound was >98% pure by HPLC analysis performed with $CH_3CN/H_2O/HCOONH_4$ (20 mM, pH = 5), 75 : 25 v/v, at a flow rate 1 mL min^{-1}.

3.3.23. (*Z*)-2-(1-(4-(6,7-Dimethoxy-3,4-dihydroisoquinolin-2(1*H*)-yl)butyl)-2-oxoindolin-3-ylidene)-*N*-(4-(trifluoromethyl)-phenyl)hydrazinecarbothioamide hydrochloride (16a). Crystallization from H_2O/EtOH afforded the title compound as a yellow solid, (0.059 g, yield 16%); mp = 155 °C (dec.); ^{1}H-NMR (500 MHz, DMSO-d_6) δ 1.73–1.84 (m, 4H, CH_2CH_2CH_2N), 2.88–2.91 (m, 1H, NCH_2C*H*HAr), 3.10–3.25 (m, 4H, CH_2NCH_2CH_2Ar), 3.55–3.63 (m, 1H, NCH_2CH*H*Ar), 3.71 (s, 3H, OCH_3), 3.72 (s, 3H, OCH_3), 3.82–3.84 (m, 2H, $CONCH_2$), 4.10–4.18 (m, 1H, NC*H*HAr), 4.35–4.40 (m, 1H, NCH*H*Ar), 6.76 (s, 1H, aromatic), 6.80 (s, 1H, aromatic), 7.20 (t, 1H, *J* = 7.34 Hz, aromatic), 7.27 (d, 1H, *J* = 7.83 Hz, aromatic), 7.48 (t, 1H, *J* = 7.83 Hz, aromatic), 7.80 (d, 2H, *J* = 8.32 Hz, aromatic), 7.86 (d, 1H, *J* = 7.34 Hz, aromatic), 7.93 (d, 2H, *J* = 8.3 Hz, aromatic), 10.64 (broad s, 1H, NH), 11.09 (s, 1H, NHAr), 12.86 (s, 1H, NH); LC-MS (ESI^+) *m*/*z*: 612 $[M + H]^+$; 634 $[M + Na]^+$; LC-MS-MS 612: 451; LC-MS-MS 634: 473; LC-MS (ESI^-) *m*/*z* 610 $[M - H]^-$; LC-MS-MS 522: 407. Compound was >98% pure by HPLC analysis performed with $CH_3CN/H_2O/HCOONH_4$ (20 mM, pH = 5), 75 : 25 v/v, at a flow rate 1 mL min^{-1}.

3.3.24. (*Z*)-2-[1-[4-(4-Cyclohexylpiperazin-1-yl)butyl]-2-oxoindolin-3-ylidene]-*N*-(4-(trifluoromethyl)phenyl)hydrazinecarbothioamide dihydrochloride (16b). Crystallization from AcOEt afforded the title compound as a red-orange solid (0.280 g, yield 75%); mp = 250 °C (dec.); ^{1}H-NMR (500 MHz, DMSO-d_6): δ 1.05–2.20 (m, 14H, cyclohexyl CH_2 and CH_2CH_2CH_2N), 3.10–3.90 (m, 13H, NCH_2, $CONCH_2$ and cyclohexyl CH), 7.13–7.17 (m, 1H, aromatic), 7.17–7.22 (m, 1H, aromatic), 7.24–7.28 (m, 1H, aromatic), 7.44–7.50 (m, 1H, aromatic), 7.78–7.82 (m, 2H, aromatic), 7.83–7.87 (m, 1H, aromatic), 7.91–7.96 (m, H, aromatic), 11.07 (s, 1H, NH), 11.60–12.00 (broad s, 2H, NH), 12.85 (s, 1H, NH); LC-MS (ESI^+) *m*/*z* 587 $[M + H]^+$; LC-MS-MS 587: 426. LC-MS (ESI^-): *m*/*z* 585 $[M - H]^-$; LC-MS-MS 585: 382. Compound was >98% pure by HPLC analysis performed with $CH_3CN/H_2O/HCOONH_4$ (20 mM, pH = 5), 75 : 25 v/v, at a flow rate 1 mL min^{-1}.

3.3.25. (*Z*)-2-(1-(4-(6,7-Dimethoxy-3,4-dihydroisoquinolin-2(1*H*)-yl)butyl)-2-oxoindolin-3-ylidene)-*N*-(naphthalen-1-yl)-hydrazinecarbothioamide hydrochloride (17a). Crystallization from H_2O/EtOH afforded the title compound as yellow solid (0.133 g, resa 37%), mp = 200 °C (dec.); ^{1}H-NMR (500 MHz, DMSO-d_6) δ 1.72–1.89 (m, 4H, CH_2CH_2CH_2N), 2.88–2.96 (m, 1H, NCH_2C*H*HAr), 3.05–3.15 (m, 4H, CH_2NCH_2CH_2Ar), 3.44–3.67 (m, 1H, NCH_2CH*H*Ar), 3.71 (s, 3H, OCH_3), 3.73 (s, 3H, OCH_3), 3.84 (t, 2H, *J* = 6.85 Hz, $CONCH_2$), 4.10–4.20 (m, 1H, NC*H*HAr), 4.35–4.42 (m, 1H, NCH*H*Ar), 6.77 (s, 1H, aromatic), 6.81 (s, 1H, aromatic), 7.18 (t, 1H, *J* = 7.8 Hz, aromatic), 7.27 (d, 1H, *J* = 7.8 Hz, aromatic), 7.47 (t, 1H, *J* = 7.8 Hz, aromatic), 7.53–7.61 (m, 4H, aromatic), 7.82–7.86 (m, 2H, aromatic), 7.96 (d, 1H, *J* = 8.3 Hz, aromatic), 8.00–8.03 (m, 1H, aromatic), 10.44 (broad s, 1H, NH), 11.19 (s, 1H, NHAr), 12.83 (s, 1H, NH); LC-MS (ESI^+) *m*/*z*: 594 $[M + H]^+$; 616 $[M + Na]^+$; LC-MS-MS 594: 451; LC-MS-MS 616: 473. Compound was >98% pure by HPLC analysis performed with $CH_3CN/H_2O/HCOONH_4$ (20 mM, pH = 5), 75 : 25 v/v, at a flow rate 1 mL min^{-1}.

3.3.26. (*Z*)-2-[1-[4-(4-Cyclohexylpiperazin-1-yl)butyl]-2-oxoindolin-3-ylidene]-*N*-(naphthalen-1-yl)hydrazinecarbothioamide dihydrochloride (17b). Crystallization from H_2O/MeOH afforded the title compound as yellow solid (0.235 g, resa 65%), mp = 250 °C (dec.); ^{1}H-NMR (500 MHz, DMSO-d_6) δ 1.00–2.20 (m, 14H, cyclohexyl CH_2 and CH_2CH_2CH_2N), 3.15–3.90 (m, 13H, NCH_2, $CONCH_2$ and cyclohexyl CH), 7.16–7.21 (m, 1H, aromatic), 7.24–7.29 (m, 1H, aromatic), 7.44–7.50 (m, 1H, aromatic), 7.53–7.63 (m, 4H, aromatic), 7.80–7.89 (m, 2H, aromatic), 7.94–7.99 (m, 1H, aromatic), 7.99–8.20 (m, 1H, aromatic), 11.13–11.28 (m, 1H, NH), 11.30–11.96 (broad s, 2H, NH), 12.72–12.89 (m, 1H, NH); LC-MS (ESI^+): *m*/*z* 569 $[M + H]^+$; LC-MS-MS 569: 426; LC-MS (ESI^-): *m*/*z* 567 $[M - H]^-$; LC-MS-MS 567: 382. Compound was >98% pure by HPLC analysis performed with $CH_3CN/H_2O/HCOONH_4$ (20 mM, pH = 5), 75 : 25 v/v, at a flow rate 1 mL min^{-1}.

3.4. Biology

3.4.1. Materials. [^{3}H]-DTG (29 Ci $mmol^{-1}$) and (+)-[^{3}H]-pentazocine (32 Ci $mmol^{-1}$) were purchased from PerkinElmer Life Sciences (Zavantem, Belgium). DTG was purchased from Tocris Cookson Ltd, U.K. (+)-Pentazocine was obtained from Sigma-Aldrich-RBI s.r.l. (Milan, Italy). Male Dunkin guinea-pigs and Wistar Hannover rats (250–300 g) were from Harlan, Italy. Cell culture reagents were purchased from EuroClone (Milan, Italy). Calcein-AM, MTT (3-[4,5-dimethylthiazol-2-yl]-2,5-diphenyltetrazoliumbromide), doxorubicin, ferrozine (3-[2-pyridyl]-5,6-diphenyl-1,2,4-triazine-4′,4″-disulfonic acid sodium salt) were obtained from Sigma-Aldrich (Milan, Italy).

3.4.2. Competition binding assays. All the procedures for the binding assays were previously described. σ_1 and σ_2 receptor binding were carried out according to Berardi *et al.*[51] The specific radioligands and tissue sources were respectively: (a) σ_1 receptor, (+)-[^{3}H]-pentazocine, guinea-pig brain membranes without cerebellum; (b) σ_2 receptor, [^{3}H]-DTG in the presence of 1 μM (+)-pentazocine to mask σ_1 receptors, rat liver membranes. The following compounds were used to define the specific binding reported in parentheses: (a) (+)-pentazocine (73–87%), (b) DTG (85–96%). Concentrations required to inhibit 50% of radioligand specific binding (IC_{50}) were determined by

using six to nine different concentrations of the drug studied in two or three experiments with samples in duplicate. Scatchard parameters (K_d and B_{max}) and apparent inhibition constants (K_i) values were determined by nonlinear curve fitting, using the Prism, version 3.0, GraphPad software (1998).[52]

3.4.3. Cell culture. MDCK-MDR1 cells was a gift of Prof. P. Borst, NKI-AVL Institute, Amsterdam, Netherland. Human MCF7 breast adenocarcinoma cells was purchased from ICLC (Genoa, Italy). Human A549 lung cancer cells was obtained from ATCC (Manassas, VA). The doxorubicin-resistant counterpart breast MCF7dx cells and lung A549dx tumor cells, were kindly provided by Prof. Chiara Riganti (Dep. of Oncology, University of Turin, Italy). MCF7 and MDCK-MDR1 cells were grown in DMEM high glucose supplemented with 10% fetal bovine serum, 2 mM glutamine, 100 U mL^{-1} penicillin, 100 μg mL^{-1} streptomycin, in a humidified incubator at 37 °C with a 5% CO_2 atmosphere. A549 cells were grown in HAM'S F12 supplemented with 10% fetal bovine serum, 2 mM glutamine, 100 U mL^{-1} penicillin, 100 μg mL^{-1} streptomycin, in a humidified incubator at 37 °C with a 5% CO_2 atmosphere. MCF7dx and A549dx were grown in the same medium of parental cells supplemented with doxorubicin (100 nM for MCF7dx and 10 nM for A549dx, respectively).

3.4.4. Calcein-AM experiment. These experiments were carried out as already described.[43] MDCK-MDR1 cell line (50 000 cells per well) was seeded into black culture plate 96/wells plate with 100 mL medium and allowed to become confluent overnight. 100 μL of different concentrations of test compounds (0.1–100 μM) were solubilized in culture medium and added to each well. The 96/wells plate was incubated at 37 °C for 30 min. 100 μL of calcein-AM, solved in Phosphate Buffered Saline (PBS), was added to each well to yield a final concentration of 2.5 μM, and the plate was incubated for 30 min. The plate was washed 3 times with 100 mL ice cold PBS. Saline buffer (100 μL) was added to each well and the plate was read by a PerkinElmer Victor3 spectrofluorimeter at excitation and emission wavelengths of 485 nm and 535 nm, respectively. In these experimental conditions, calcein cell accumulation in the absence and in the presence of tested compounds was evaluated and fluorescence basal level was estimated by untreated cells. In treated wells the increase of fluorescence with respect to basal level was measured. EC_{50} values were determined by fitting the fluorescence increase percentage *versus* log[dose].

3.4.5. Bioluminescent ATP assay. This experiment was performed as reported in technical sheet of ATPlite 1 step Kit for luminescence ATP detection based on firefly (*Photinus pyralis*) luciferase (PerkinElmer Life Sciences).[53] The ATPlite assay is based on the production of light caused by the reaction of ATP with added luciferase and D-luciferin (substrate solution) and the emitted light is proportional to the ATP concentration. The MDCK-MDR1 cells were seeded into black culture plate 96/wells plate in 100 μL of complete medium at a density 2×10^4 cells per well. The plate was incubated O/N in a humidified atmosphere 5% CO_2 at 37 °C. The medium was removed and 100 μL of complete medium in the presence or absence of different concentrations of test compounds was added. The plate was incubated for 2 h in a humidified atmosphere 5% CO_2 at 37 °C. Then, 50 μL of mammalian cell lysis solution was added to all wells and the plate stirred for 5 minutes in an orbital shaker. In all wells, 50 μL of substrate solution was added and the plate stirred for 5 min in an orbital shaker. The plate was dark adapted for 10 min and the luminescence was measured on the microplate reader Victor 3 from PerkinElmer Life Sciences.

3.4.6. Iron chelation assay. This assay are performed as reported in Viollier *et al.*,[54] with minor modification. Ferrozine reacts with divalent iron to form stable magenta species. The maximum absorbance is recorded at a wavelength of 562 nm. To confirm the chelation properties of our thiosemicarbazone compounds, we incubated the standard curve of $FeSO_4$ in presence or absence of our compounds. Ferrozine stock solution was prepared at 10^{-2} M in water. $FeSO_4$ standard solution was prepared at 10^{-2} M in water. Tested compounds stock solution was prepared at 10^{-2} M in DMSO. 1 mL of $FeSO_4$ standard curve (0.5–25 μM) was incubated with or without 10 μL of tested compound (100 μM) for 15 min at room temperature. 10 μL of ferrozine (100 μM) was added and the solution was analyzed at the UV/Vis spectrophotometer at wavelengths of 562 nm.

3.4.7. Cell viability. Determination of cell growth was performed using the MTT assay at 48 h.[55] On day 1, 25 000 cells per well were seeded into 96-well plates in a volume of 100 μL. On day 2, the various drugs concentration (1–100 μM) were added. In all the experiments, the various drug-solvents (EtOH, DMSO) were added in each control to evaluate a possible solvent cytotoxicity. After the established incubation time with drugs (48 h), MTT (0.5 mg mL^{-1}) was added to each well, and after 3–4 h incubation at 37 °C, the supernatant was removed. The formazan crystals were solubilized using 100 μL of DMSO/EtOH (1 : 1) and the absorbance values at 570 and 630 nm were determined on the microplate reader Victor 3 from PerkinElmer Life Sciences. The interference of ROS in cell viability was indirectly determined by MTT assay reported above at 24 h. On day 1, 25 000 cells per well were seeded into 96-well plates in the presence or absence of α-tocopherol (100 μM). On day 2, the drugs (1–100 μM) were added alone and in combination with α-tocopherol (100 μM). After incubation (24 h) with drugs, MTT assay was performed as above.

4. Conclusions

There is a desperate need for effective strategies to treat MDR. The availability of novel and promising molecules to be studied for fighting resistant tumors was widen through this work. For the first time molecules targeting simultaneously σ_2 and Pg-p proteins (two hallmarks of proliferating and resistant tumors) while sequestering iron species, were generated with the aim to hit P-gp overexpressing tumors. Several antiproliferative agents with potent activity in breast and lung doxorubicin resistant cells were obtained. Some of them hold promises for the treatment of resistant tumors and deserve deeper characterization. Also, the present work sets up the stage for further studies that aim at clarifying the contribution of each target to the overall effects of these compounds as well as the activated

pathways so that more potent and selective molecules may be produced to combat the emergence of resistant tumors.

References

1 W. R. Martin, C. G. Eades, J. A. Thompson, R. E. Huppler and P. E. Gilbert, *J. Pharmacol. Exp. Ther.*, 1976, **197**, 517–532.

2 M. Hanner, F. F. Moebius, A. Flandorfer, H. G. Knaus, J. Striessnig, E. Kempner and H. Glossmann, *Proc. Natl. Acad. Sci. U. S. A.*, 1996, **93**, 8072–8077.

3 L. Nguyen, B. P. Lucke-Wold, S. A. Mookerjee, J. Z. Cavendish, M. J. Robson, A. L. Scandinaro and R. R. Matsumoto, *J. Pharmacol. Sci.*, 2015, **127**, 17–29.

4 S. Y. Tsai, M. J. Pokrass, N. R. Klauer, H. Nohara and T. P. Su, *Proc. Natl. Acad. Sci. U. S. A.*, 2015, **112**, 6742–6747.

5 A. A. Behensky, I. E. Yasny, A. M. Shuster, S. B. Seredenin, A. V. Petrov and J. Cuevas, *J. Pharmacol. Exp. Ther.*, 2013, **347**, 468–477.

6 T. A. Mavlyutov, L. W. Guo, M. L. Epstein and A. E. Ruoho, *J. Pharmacol. Sci.*, 2015, **127**, 10–16.

7 A. Al-Saif, F. Al-Mohanna and S. Bohlega, *Ann. Neurol.*, 2011, **70**, 913–919.

8 C. Moritz, F. Berardi, C. Abate and F. Peri, *Neurosci. Lett.*, 2015, **591**, 13–18.

9 A. A. Hall, Y. Herrera, C. T. Ajmo Jr, J. Cuevas and K. R. Pennypacker, *Glia*, 2009, **57**, 744–754.

10 N. A. Colabufo, F. Berardi, C. Abate, M. Contino, M. Niso and R. Perrone, *J. Med. Chem.*, 2006, **49**, 4153–4158.

11 C. Abate, J. Elenewski, M. Niso, F. Berardi, N. A. Colabufo, A. Azzariti, R. Perrone and R. A. Glennon, *ChemMedChem*, 2010, **5**, 268–273.

12 J. Xu, C. Zeng, W. Chu, F. Pan, J. M. Rothfuss, F. Zhang, Z. Tu, D. Zhou, D. Zeng, S. Vangveravong, F. Johnston, D. Spitzer, K. C. Chang, R. S. Hotchkiss, W. G. Hawkins, K. T. Wheeler and R. H. Mach, *Nat. Commun.*, 2011, **2**, 380.

13 C. Abate, M. Niso, V. Infantino, A. Menga and F. Berardi, *Eur. J. Pharmacol.*, 2015, **758**, 16–23.

14 R. H. Mach, C. Zeng and W. G. Hawkins, *J. Med. Chem.*, 2013, **56**, 7137–7160.

15 S. V. Selivanova, A. Toscano, C. Abate, F. Berardi, A. Müller, S. D. Krämer, R. Schibli and S. M. Ametamey, *Nucl. Med. Biol.*, 2015, **42**, 399–405.

16 ClinicalTrials.gov Identifier: NCT00968656. Phase I Clinical Trial. Assessment of cellular proliferation in tumors by Positron Emission Tomography (PET) using [^{18}F]ISO-1 (FISO PET/CT).

17 ClinicalTrials.gov Identifier: NCT02284919. Imaging of *In Vivo* Sigma-2 Receptor Expression With [^{18}F]ISO-1 Positron Emission Tomography (PET/CT) in Primary Breast Cancer.

18 C. Abate, R. Perrone and F. Berardi, *Curr. Pharm. Des.*, 2012, **18**, 938–949.

19 J. R. Hornick, S. Vangveravong, D. Spitzer, C. Abate, F. Berardi, P. Goedegebuure, R. H. Mach and W. G. Hawkins, *J. Exp. Clin. Cancer Res.*, 2012, **31**, 41.

20 Y. M. Hashim, D. Spitzer, S. Vangveravong, M. C. Hornick, G. Garg, J. R. Hornick, P. Goedegebuure, R. H. Mach and W. G. Hawkins, *Mol. Oncol.*, 2014, **8**, 956–967.

21 Y. S. Huang, H. L. Lu, L. J. Zhang and Z. Wu, *Med. Res. Rev.*, 2014, **34**, 532–566.

22 C. Abate, P. D. Mosier, F. Berardi and R. A. Glennon, *Cent. Nerv. Syst. Agents Med. Chem.*, 2009, **9**, 246–257.

23 D. J. Rhoades, D. H. Kinder and T. M. Mahfouz, *Med. Chem.*, 2014, **10**, 98–121.

24 S. Ferorelli, C. Abate, N. A. Colabufo, M. Niso, C. Inglese, F. Berardi and R. Perrone, *J. Med. Chem.*, 2007, **50**, 4648–4655.

25 C. Abate, J. R. Hornick, D. Spitzer, W. J. Hawkins, M. Niso, R. Perrone and F. Berardi, *J. Med. Chem.*, 2011, **54**, 5858–5867.

26 C. Abate, M. Niso, R. Marottoli, C. Riganti, D. Ghigo, S. Ferorelli, G. Ossato, R. Perrone, E. Lacivita, D. C. Lamb and F. Berardi, *J. Med. Chem.*, 2014, **57**, 3314–3323.

27 M. Niso, C. Riganti, M. L. Pati, D. Ghigo, F. Berardi and C. Abate, *ChemBioChem*, 2015, **16**, 1078–1083.

28 R. H. Mach and K. T. Wheeler, *Cent. Nerv. Syst. Agents Med. Chem.*, 2009, **9**, 230–245.

29 C. Zeng, S. Vangveravong, L. A. Jones, K. Hyrc, K. C. Chang, J. Xu, J. M. Rothfuss, M. P. Goldberg, R. S. Hotchkiss and R. H. Mach, *Mol. Imaging*, 2011, **10**, 420–433.

30 B. Schininà, A. Martorana, N. A. Colabufo, M. Contino, M. Niso, M. G. Perrone, G. de Guidi, A. Catalfo, G. Rappazzo, E. Zuccarello, O. Prezzavento, E. Amata, A. Rescifina and A. Marrazzo, *RSC Adv.*, 2015, **5**, 47108–47113.

31 C. Zeng, J. Rothfuss, J. Zhang, W. Chu, S. Vangveravong, Z. Tu, F. Pan, K. C. Chang, R. Hotchkiss and R. H. Mach, *Br. J. Cancer*, 2012, **106**, 693–701.

32 S. U. Mir, S. R. Schwarze, L. Jin, J. Zhang, W. Friend, S. Miriyala, D. S. Clair and R. J. Craven, *Autophagy*, 2013, **9**, 1566–1578.

33 M. Niso, C. Abate, M. Contino, S. Ferorelli, A. Azzariti, R. Perrone, N. A. Colabufo and F. Berardi, *ChemMedChem*, 2013, **8**, 2026–2035.

34 M. Niso, C. Abate and C. Riganti, *Recept. Clin. Investig.*, 2014, **1**, 208–216.

35 K. M. Pluchino, M. D. Hall, A. S. Goldsborough, R. Callaghan and M. M. Gottesman, *Drug Resist. Updates*, 2012, **15**, 98–105.

36 M. D. Hall, K. R. Brimacombe, M. S. Varonka, K. M. Pluchino, J. K. Monda, J. Li, M. J. Walsh, M. B. Boxer, T. H. Warren, H. M. Fales and M. M. Gottesman, *J. Med. Chem.*, 2011, **54**, 5878–5889.

37 D. R. Richardson, P. C. Sharpe, D. B. Lovejoy, D. Senaratne, D. S. Kalinowski, M. Islam and P. V. Bernhardt, *J. Med. Chem.*, 2006, **49**, 6510–6521.

38 J. Yuan, D. B. Lovejoy and D. R. Richardson, *Blood*, 2004, **104**, 1450–1458.

39 C. Abate, S. Ferorelli, M. Contino, R. Marottoli, N. A. Colabufo, R. Perrone and F. Berardi, *Eur. J. Med. Chem.*, 2011, **46**, 4733–4741.

40 C. Abate, S. V. Selivanova, A. Müller, S. D. Krämer, R. Schibli, R. Marottoli, R. Perrone, F. Berardi, M. Niso and S. M. Ametamey, *Eur. J. Med. Chem.*, 2013, **69**, 920–930.

41 S. Bai, S. Li, J. Xu, X. Peng, K. Sai, W. Chu, Z. Tu, C. Zeng and R. H. Mach, *J. Med. Chem.*, 2014, **57**, 4239–4251.

42 M. D. Hall, N. K. Salam, J. L. Hellawell, H. M. Fales, C. B. Kensler, J. A. Ludwig, G. Szakács, D. E. Hibbs and M. M. Gottesman, *J. Med. Chem.*, 2009, **52**, 3191–3204.
43 C. Abate, M. L. Pati, M. Contino, N. A. Colabufo, R. Perrone, M. Niso and F. Berardi, *Eur. J. Med. Chem.*, 2015, **89**, 606–615.
44 Y. Yu, Y. S. Rahmanto and D. R. Richardson, *Br. J. Pharmacol.*, 2012, **165**, 148–166.
45 C. R. Kowol, R. Trondl, P. Heffeter, V. B. Arion, M. A. Jakupec, A. Roller, M. Galanski, W. Berger and B. K. Keppler, *J. Med. Chem.*, 2009, **52**, 5032–5043.
46 D. S. Kalinowski, P. C. Sharpe, P. V. Bernhardt and D. R. Richardson, *J. Med. Chem.*, 2007, **50**, 6212–6225.
47 D. S. Kalinowski, Y. Yu, P. C. Sharpe, M. Islam, Y.-T. Liao, D. B. Lovejoy, N. H. Kumar, P. V. Bernhardt and D. R. Richardson, *J. Med. Chem.*, 2007, **50**, 3716–3729.
48 M. Whitnall, J. Howard, P. Ponka and D. R. Richardson, *Proc. Natl. Acad. Sci. U. S. A.*, 2006, **103**, 14901–14906.
49 R. Trondl, L. S. Flocke, C. R. Kowol, P. Heffeter, U. Jungwirth, G. E. Mair, R. Steinborn, É. A. Enyedy, M. A. Jakupec, W. Berger and B. K. Keppler, *Mol. Pharmacol.*, 2014, **85**, 451–459.
50 P. Heffeter, C. Pirker, C. R. Kowol, G. Herrman, R. Dornetshuber, W. Miklos, U. Jungwirth, G. Koellensperger, B. K. Keppler and W. Berger, *Biochem. Pharmacol.*, 2012, **83**, 1623–1633.
51 F. Berardi, C. Abate, S. Ferorelli, V. Uricchio, N. A. Colabufo, M. Niso and R. Perrone, *J. Med. Chem.*, 2009, **52**, 7817–7828.
52 *Prism Software, version 3.0 for Windows*, GraphPad Software, Inc., San Diego, CA, 1998.
53 N. A. Colabufo, F. Berardi, M. Cantore, M. G. Perrone, M. Contino, C. Inglese, M. Niso, R. Perrone, A. Azzariti, G. M. Simone, L. Porcelli and A. Paradiso, *Bioorg. Med. Chem.*, 2008, **16**, 362–373.
54 E. Viollier, P. W. Inglett, K. Hunter, A. N. Roychoudhury and P. van Cappellen, *Appl. Geochem.*, 2000, **15**, 785–790.
55 N. A. Colabufo, F. Berardi, M. Contino, M. Niso, C. Abate, R. Perrone and V. Tortorella, *Naunyn-Schmiedeberg's Arch. Pharmacol.*, 2004, **370**, 106–113.